the isolates can be found elsewhere (Coatney et al., 1971). All the primate malaria strains were provided by the Centers for Disease Control and Prevention. The sequences reported in this study are deposited in the GenBank with the accession numbers DQ907617–DQ907702.

2.1. Statistical analysis

We estimate genetic polymorphism by using the parameter π, which estimates the average number of substitutions between any two sequences. The average number of synonymous (Ds) and non-synonymous substitutions (Dn) between a pair of sequences was investigated to explore the effect of natural selection. The average numbers of synonymous and non-synonymous substitutions are estimated using two methods: Nei and Gojobori's method (1986) with the Jukes and Cantor correction, and the Li's method (1993) as implemented in the MEGA program (Kumar et al., 2001). We estimated the difference between Ds and Dn, its standard deviation was calculated using bootstrap with 1000 pseudo-replications for Ds and Dn, as well as a two tail Z-test on the difference between Ds and Dn (Nei and Kumar, 2000). The null hypothesis is that Ds = Dn; thus, we assumed as null hypothesis that the observed polymorphism was neutral.

The Tajima's D statistic and F^* from Fu and Li were estimated for testing the hypothesis that the allele frequency spectrum is compatible with the neutral model (Tajima, 1989; Fu and Li, 1993). Under the neutral model, Tajima's D and F^* are approximately equal to zero, thus any deviation from zero would indicate a departure from neutrality in the allele frequency spectrum.

Evidence for recombination was assessed by using the Rm parameter that estimates the minimum number of recombination events in the history of the sample. Rm is obtained using the four-gamete test (Hudson and Kaplan, 1985) and, as the name of the parameter indicates, it is a conservative estimate of the number of recombination events.

In the case of *P. vivax* and related non-human primate malarial parasites, the gene genealogy of the MSP-1_{42} alleles was determined by using the Neighbor–Joining (Saitou and Nei, 1987) method with the Tamura-Nei model. The reliability of the nodes in the NJ tree was assessed by the bootstrap method with 1000 pseudo-replications. The genealogy was estimated using the MEGA program (Kumar et al., 2001). The assumption of neutrality was also tested in *P. vivax* MSP-1 by using the McDonald and Kreitman test (McDonald and Kreitman, 1991), which compares the intra-and interspecific number of synonymous and non-synonymous sites; significance was assessed by using a Fishers exact test for the 2 × 2 contingency table as implemented in the programs DNAsp Version 4.0 (Rozas et al., 2003). In this analysis, we compare *P. vivax* with *P. cynomolgi* and *P. inui* (see below).

3. Results

Table 1 shows the genetic diversity found in the MSP-1_{42} fragments in *P. falciparum* and *P. vivax*. Overall, the genetic diversity of *P. falciparum* is twice that observed in *P. vivax* (π of 0.05042 versus 0.02184). Analysis of the genetic diversity of the MSP-1_{33} and MSP-1_{19} fragments confirmed previous observations that the MSP-1_{19} fragment is more conserved than the MSP-1_{33} fragment (Table 1) in both human malarial parasites. *P. vivax* MSP-1_{19} has only one polymorphic site while in *P. falciparum* the substitutions are concentrated in five residues within the epidermal growth factor like domains (EGF). In an extended alignment that included all the MSP-1_{19} sequences reported in the literature at the time of this study ($n = 175$); we found 11 alleles reported based in these five residues, among them, there are four common alleles that have a worldwide distribution: E-KNG-L ($n = 54$), E-TSR-L ($n = 41$), Q-KNG-F ($n = 20$), Q-KNG-L ($n = 33$). It is worth noting that some alleles, although reported in low frequency, have been found in two continents; such are the cases of E-KNG-F ($n = 8$ reported in India and Kenya), E-KSR-L ($n = 4$ reported in Kenya, South Africa, and Vanuatu), and Q-TSR-L ($n = 3$ reported in India and Papua New Guinea). The allele E-TSG-L ($n = 9$) has been reported three times in India (including this study) and is the one observed in *P. reichenowi*, the most closely related species to *P. falciparum* found in chimpanzees (Coatney et al., 1971).

We found two recombination-convergent events using the Rm method (Hudson and Kaplan, 1985); these events are

Table 1
Polymorphism found in the MSP-1_{42} in *P. falciparum* and *P. vivax*

	π	Ds	Dn	Ds − Dn (S.D.)	Z	Tajima D	F^*
P. falciparum ($n = 120$)							
42 KDa	0.05042	0.0821	0.0541	0.0280 (0.011)	Ds > Dn ($P<0.05$)	−0.11184 n.s.	0.13353 n.s.
33 KDa	0.06551	0.1236	0.0741	0.0494 (0.020)	Ds > Dn ($P<0.05$)	0.10150 n.s.	0.86091 n.s.
19 KDa	0.00884	0.0013	0.0107	−0.009 (0.004)	Ds < Dn ($P<0.05$)	−1.72070 ($0.10>P>0.05$)	−4.78810 ($P<0.05$)
P. vivax ($n = 75$)							
42 KDa	0.02184	0.0125	0.0249	−0.0123 (0.005)	Ds < Dn ($P<0.05$)	2.19241 ($P<0.05$)	2.09599 ($P<0.05$)
33 KDa	0.03249	0.0162	0.0325	−0.0160 (0.006)	Ds < Dn ($P<0.05$)	2.31357 ($P<0.05$)	2.24458 ($P<0.05$)
19 KDa	0.0006	0.0005	0.0006	0.0001 (0.000)	Ds = Dn	−1.02018 n.s	−1.02018 n.s

π, nucleotide diversity; n, number of sequences; Dn is the nucleotide diversity of non-synonymous mutations per non-synonymous sites and Ds is the nucleotide diversity of synonymous mutations per synonymous site using the Nei and Gojobori method; Ds − Dn are the difference of Ds and Dn with their standard deviation, SD, estimated by bootstrap with 1000 pseudo replicates; Z is the Z-test (Nei and Kumar, 2000); Tajima D and F^* are tests for detecting departures from the neutral model.

illustrated using the relative positions of the residues in the allele E-KNG-L, specifically between the position held by the amino acids E and K (separated by 138 bp) and between the positions filled by amino acids K and G (separated by 30 bp). Recombination events have been previously reported in MSP-1_{19} (Qari et al., 1998).

In order to explore the role of natural selection we further analyzed the genetic polymorphism in the MSP-1_{42} as a unit by estimating the number of synonymous (Ds) and non-synonymous (Dn) substitutions per site estimated by the Nei and Gojobori method with the Jukes and Cantor correction. When this comparison is made, both parasites exhibit opposite patterns: MSP-1_{42} in *P. falciparum* shows more synonymous than non-synonymous substitutions while the homologous region in *P. vivax* shows more non-synonymous than synonymous substitutions. In both cases the differences are significant with a Z-test (Nei and Kumar, 2000) (Table 1). The Li's method gives identical results. We explore departure from neutrality by using the Tajima's *D* test (Tajima, 1989) and F^* test (Fu and Li, 1993). These tests should to be used with caution since they aim to detect departures from a neutral panmictic population, an assumption that is violated by these geographically and temporally spaced samples. Nevertheless, we used them to explore the distribution of haplotypes in our samples as was used previously to compare *P. vivax* and *P. knowlesi* (Putaporntip et al., 2006). These tests could not detect departure from neutrality in *P. falciparum*, although they did so in *P. vivax* when the complete MSP-1_{42} was considered as a unit.

We explored the diversity in the MSP-1_{33} and MSP-1_{19} fragments separately by comparing the number of synonymous and non-synonymous substitutions in each species. In the case of the MSP-1_{33} of *P. falciparum* there are more synonymous than non-synonymous substitutions ($P < 0.05$) (Table 1), while the contrary was observed in the MSP-1_{19} where there are more non-synonymous than synonymous substitutions ($P < 0.05$). These results suggest that while the MSP-1_{19} is under positive selection in *P. falciparum*, the MSP-1_{33} is under purifying selection; that is, natural selection favors the maintenance of amino acid polymorphism in the MSP-1_{19} while it holds back the rate of amino-acid polymorphism in the MSP-1_{33}. Differences between the MSP-1_{33} and MSP-1_{19} were also observed by using the Tajima's *D* and F^* tests (Table 1): there is not a departure from neutrality in the MSP-1_{33} while the MSP-1_{19} polymorphism rejects the expectation under the neutral model. Although the significance level by the Tajima's *D* test is weak for MSP-1_{19} ($0.05 < P < 0.1$), there is almost no synonymous variation, substantiating a departure from the neutrality in this region. It is important to notice that the Tajima's *D* and F^* tests have a negative value indicating that there is an excess of low frequency variants in the sample (Table 1).

In the case of *P. vivax* the pattern is the opposite. There are more non-synonymous than synonymous substitutions in the MSP-1_{33} while there is almost no variation in the MSP-1_{19} (Table 1). The polymorphism in the *P. vivax* MSP-1_{33} is not evenly distributed. Indeed, there is a region of 105 bp out of 848 bp in MSP-1_{33} (35 amino acids) where a clear excess of non-synonymous versus synonymous substitution is observed driving the overall MSP-1_{33} results. In addition, there is a departure from neutrality in the MSP-1_{33} when the Tajima's *D* and F^* tests are applied. However, contrasting with *P. falciparum*, the value of the test is positive as the result of an excess of variants in intermediate frequencies.

We further explore the hypothesis that positive selection is acting on the *P. vivax* MSP-1_{33} fragment by comparing it with its closely related non-human primate malarial parasites (Escalante et al., 2005). The genealogy of the MSP-1_{42} fragments from the species reported in this study is depicted in Fig. 1. *P. cynomolgi* appears as sister taxa of *P. vivax*; however, this clade does not have strong support. *P. cynomolgi* strains are subdivided into two clear clades; no evidence for allele families could be observed with this fragment. *P. inui* and *P. hylobati* are closely related as previously reported (Escalante et al., 2005). The close relationship of these two species was further supported by the presence of a repetitive sequence in the MSP-1_{33} fragment. Specifically, a motif with the residues NE*QEEI* is inserted in some of the *P. inui* isolates while *P. hylobati* has the residues NE*QEEI*KIR*QEEI*. We also found an insertion in *P. knowlesi* that emerged as a duplication of the motif *INNCQIEK* conserved in *P. inui* and *P. vivax* (Fig. 2). Given the lack of

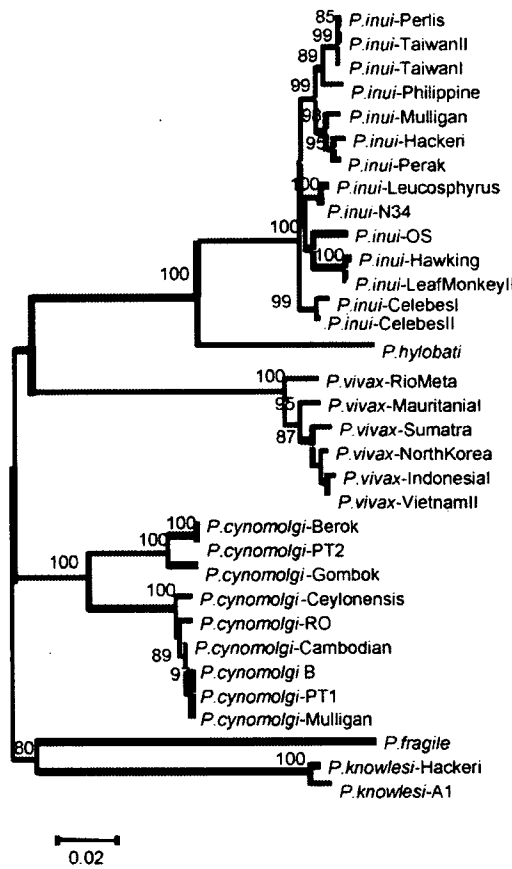

Fig. 1. Neighbor–Joining tree of the MSP-1_{42} alleles using Tamura-Nei's distance. The numbers on the nodes of the tree are percent of bootstrap values based on 1000 pseudo-replications. The sequences reported in this study are identified with their species and strain names.

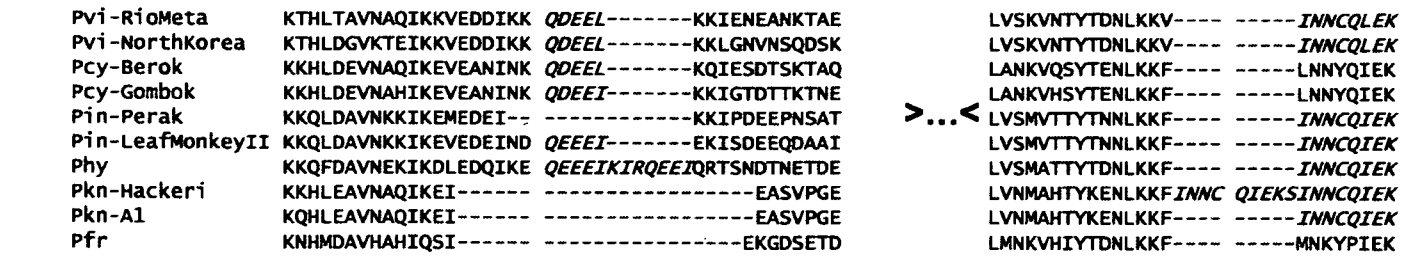

Fig. 2. Repetitive sequences observed in the MSP-1_{42}. The observed motifs are in italics. The dots (>...<) are indicating a non-repetitive portion of the protein that is not shown. The first three letters in the sequence codes indicate the species: Pvi, *P. vivax*; Pcy, *P. cynomolgi*; Pin, *P. inui*; *Phy*, *P. hylobati*; Pkn, *P. knowlesi*; Pfr, *P. fragile*.

Table 2
Polymorphism found in the MSP-1_{42} in other non-human *Plasmodium* spp.

	π	Ds	Dn	Ds − Dn (S.D.)	Z
P. cynomolgi (n = 10)					
42 KDa	0.03805	0.0871	0.0287	0.0585 (0.015)	Ds > Dn (P<0.05)
33 KDa	0.06551	0.1001	0.0312	0.0687 (0.018)	Ds > Dn (P<0.05)
19 KDa	0.02502	0.0469	0.0211	0.0257 (0.022)	Ds = Dn
P. inui (n = 15)					
42 KDa	0.02416	0.0284	0.0237	0.0049 (0.006)	Ds = Dn
33 KDa	0.02951	0.0358	0.0289	0.0071 (0.008)	Ds = Dn
19 KDa	0.0067	0.0051	0.0073	−0.0022 (0.005)	Ds = Dn

π, nucleotide diversity; n, number of sequences; Dn is the nucleotide diversity of non-synonymous mutations per non-synonymous sites and Ds is the nucleotide diversity of synonymous mutations per synonymous site using the Nei and Gojobori method. Ds − Dn are the difference of Ds and Dn with their standard deviation, S.D., estimated by bootstrap with 1000 pseudo replicates. Z is the Z-test (Nei and Kumar, 2000).

resolution of the phylogeny using this region, we used both *P. cynomolgi* and *P. inui* for comparison with *P. vivax*.

Table 2 shows the basic statistics for the MSP-1_{42} in these two non-human primate malarial parasites. As in the cases of the human parasites, the MSP-1_{33} fragment is more diverse than the MSP-1_{19}. However, in the case of the non-human primate malarias, there is no excess of non-synonymous substitutions over synonymous substitutions in the MSP-1_{42} as a unit or considering the MSP-1_{33} and MSP-1_{19} fragments separated. Thus, by comparing the rate of non-synonymous versus synonymous substitutions we could not detect evidence for positive selection acting on *P. cynomolgi* or *P. inui* MSP-1_{42}. An identical pattern can be observed in *P. knowlesi* when the two complete MSP-1_{42}, the one reported in this investigation and the one available in literature (Putaporntip et al., 2006) are compared, specifically Ds = 0.04275 and Dn = 0.00240 for MSP-1_{42}.

We then analyzed the genetic diversity of *P. vivax* MSP-1_{42} by using the McDonald and Kreitman test (McDonald and Kreitman, 1991) and compared it with both *P. cynomolgi* and *P. inui* samples. In the case of the complete 42 Kda, there was an overall excess of non-synonymous over synonymous in the *P. vivax* polymorphism when compared with *P. cynomolgi* ($p < 0.05$ using a Fisher's exact test). Similar results were found with *P. vivax* and *P. inui* ($p < 0.001$ using a Fisher's exact test). In both cases, the significance of the MK test was explained by an excess of amino acid replacements in the polymorphism of the *P. vivax* MSP-1_{33}. It is worth noting that no departure from neutrality was found when only MSP1_{19} was considered. It is also important to emphasize that no departure from neutrality was observed when *P. cynomolgi* and *P. inui* were compared considering the MSP-1_{42} as a unit, or separating it into the MSP-1_{33} and MSP-1_{19} fragments.

4. Discussion

The available data, mostly derived from *P. falciparum*, indicate the importance of the antibody response against block 2 (located in the 83 kDa or MSP-1_{83}) and the MSP-1_{42} fragments in developing protective immunity. In this study, we have described the selective forces operating on the polymorphism observed in the MSP-1_{42} fragment in the two major human malaria parasites. We have shown how the MSP-1_{33} and MSP-1_{19} fragments are under different selective pressures in each of the major human malarial parasites by using the rate of non-synonymous versus synonymous substitutions.

In the case of *P. falciparum*, the polymorphism in MSP-1_{33} appears to be neutral or under purifying selection while the polymorphism in MSP-1_{19} is under positive selection. In this case, our results are consistent with immunologic evidence suggesting that the MSP-1_{19} but not MSP-1_{33} elicits a protective immune response, though the latter being highly immunogenic (Ahlborg et al., 2002). Positive selection has been previously proposed as an important mechanism in maintaining the *P. falciparum* MSP-1 polymorphism in the form of balancing selection (Hughes, 1992; Conway et al., 2000); that is, natural selection maintains genetic polymorphism for a longer time than expected under a scenario where only

genetic drift is acting. A polymorphism under balancing selection is expected to have an excess of alleles in intermediate frequencies, a pattern that translates into positives Tajima's D and F^* tests. In the case of MSP-1_{19}, however, there is an excess of alleles in low frequency as evidenced by significant and negative values of the Tajima's D and F^* tests, not consistent with balancing selection. This could be the result of several factors. First, we found four alleles that are particularly common while several others are found in low frequency in our sample; low frequency alleles that are found even in different continents suggest an artifact due to a poor sampling effort. Indeed, lack of appropriate sampling could generate negative Tajima's D tests as a result of several sub-populations being analyzed together (Hammer et al., 2003). A second alternative is that a limited number of alleles are increasing in frequency, a scenario expected under a population expansion which coincides with the results reported for mitochondrial data (Joy et al., 2003).

Nevertheless, if the population demographic history and inappropriate sampling were the only factors leading to this result (significant and negative Tajimas's D and F^* tests), then the MSP-1_{33} should have shown a similar trend. The Tajimas's D and F^* tests for MSP-1_{33} are not only non-significant but also have an opposite sign. Interestingly, the MSP-1_{33} also shows more synonymous than non-synonymous substitutions. Therefore, we propose that the negative Tajimas's D and F^* tests, together with the excess of non-synonymous over synonymous substitutions in MSP-1_{19}, are the result of directional selection, that is, there are few MSP-1_{19} alleles increasing in frequency because they are positively selected.

Although the immune response against *P. falciparum* MSP-1_{19} is still under intense investigation, there is evidence suggesting that fine specificity rather than prevalence could be an important factor in the observed immune reactivity (Okech et al., 2004). Indeed, only partial cross-reactivity has been found in holoendemic areas among the most common MSP-1_{19} alleles (Udhayakumar et al., 1995; Shi et al., 1996; John et al., 2004). It has been also shown that immunity against MSP-1_{19} in *P. falciparum* has a short lifespan to the extent that its elicited antibody responses allow detecting differences in local transmission (Drakeley et al., 2005). Therefore, the pattern in the genetic polymorphism of MSP-1_{19} could be the result of differences of the most common alleles in their specificity and/or life spans of their elicited immune responses when compared with the less frequent MSP-1_{19} alleles, differences that give them a selective advantage favoring their transmission.

Our hypothesis that directional selection is operating on MSP-1_{19} does not contradict previous claims for balancing selection since they are well supported by the extensive divergence observed in MSP-1_{83}, MSP-1_{30}, and MSP-1_{38} fragments allowing the identification of two very distinctive allele families (Tanabe et al., 1987) that have been found to be an ancient polymorphism (Hughes, 1992; Polley et al., 2005) as well as evidence derived from population base studies of the MSP-1_{83} (Conway et al., 2000; Takala et al., 2006). Indeed such divergent allele families are not observed when only the MSP-1_{19} is considered.

In the case of *P. vivax*, however, the MSP-1_{33} and MSP-1_{19} fragments appear to be under different selective pressures than the ones just described in the homologous region in *P. falciparum*. We observed an excess of non-synonymous over synonymous substitutions in the MSP-1_{33} and not in the MSP-1_{19}; in addition, we found that the Tajimas's D and F^* tests are significant and positive for MSP-1_{33}, which is expected under the scenario of balancing selection although it could be the result of population structure, a clear possibility given the origin of the sample analyzed. Nevertheless, when we studied the genetic variation in the MSP-1_{33} and MSP-1_{19} by using the McDonald and Kreitmant test against *P. cynomolgi* and *P. inui* we found an excess of non-synonymous substitutions in the *P. vivax* MSP-1_{33} no matter which species we used to compare it with, suggesting that positive natural selection is operating in this fragment.

Our results support previous observations that *P. vivax* MSP-1_{33} could play an important role in reticulocyte invasion (Espinosa et al., 2003; Rodríguez et al., 2002). However, the polymorphism in the *P. vivax* MSP-1_{33} appears more complicated; indeed, there is a 105 bp fragment with high polymorphism located between regions where peptides with high specific binding activity (HSBA) to reticulocytes have been found (Espinosa et al., 2003; Rodríguez et al., 2002). These regions with HSBA are not only highly conserved among *P. vivax* isolates ($n = 75$) but also show more synonymous than non-synonymous substitutions when compared with *P. cynomolgi* (peptides 1735, 1738 and 1747 *sensu* Rodríguez et al., 2002 have Ks of 0.30, 0.31 and 0.22 versus Kn of 0.16, 0.025, and 0.11, respectively) and a similar pattern is observed when compared with *P. inui* (peptides 1735, 1738 and 1747 *sensu* Rodríguez et al., 2002 have Ks of 0.29, 0.37, and 0.041 versus Kn of 0.17, 0.10, and 0.16, respectively). This overall pattern indicates that these HSBA regions are under selective constraints to accumulate amino acid replacements; as a result, they could be a valuable target for a vaccine against *P. vivax* as has been suggested previously (Espinosa et al., 2003).

There is no information regarding the immunologic role played by the variation observed in *P. vivax* MSP-1_{33}. Elucidating whether it hampers effective natural immune responses against these conserved regions with HSBA to reticulocytes or whether it plays any other role requires further investigation. Nevertheless, it seems clear from this comparative analyses that we cannot simply extrapolate information derived from *P. falciparum* into *P. vivax* in the case of MSP-1_{42}.

In summary, we have investigated the genetic diversity of the sequence encoding the MSP-1_{42} in the two major human malarial parasites. We found evidence supporting positive natural selection as an important factor in the maintenance and generation of the observed polymorphism. However, we describe how natural selection is acting differently in the MSP-1_{33} and MSP-1_{19} fragments of the MSP-1_{42} in each of the two human malarial parasites. That is, our results suggest that these fragments, MSP-1_{33} and MSP-1_{19}, could play different roles in each of the two human malarial parasites.

Acknowledgements

This research is supported by grants from the National Institutes of Health (R01 GM60740) to A.A.E. and from the Japanese Ministry of Education, Culture, Sports, Science and Technology (14021125) to K.T. We thank Andrea McCollum and two anonymous reviewers for their commentaries that improved this manuscript. The findings and conclusions in this report are those of the author(s) and do not necessarily represent the views of the Centers for Disease Control and Prevention.

References

Ahlborg, N., Ling, I.T., Howard, W., Holder, A.A., Riley, E.M., 2002. Protective immune responses to the 42-hilodalton (kDa) region of *Plasmodium yoelii* merozoite surface protein 1 are induced by the C-terminal 19-kDa region but not by large adjacent 33-kDa region. Infect. Immun. 70, 820–825.

Chang, S.P., Kramer, K.J., Yamaga, K.M., Kato, A., Case, S.E., Siddiqui, W.A., 1988. *Plasmodium falciparum*: Gene structure and hydropathy profile of the major merozoite surface antigen (gp195) of the Uganda-Palo Alto isolate. Exp. Parasitol. 67, 1–11.

Chitnis, C.E., Miller, L.H., 1994. Identification of the erythrocyte binding domains of *Plasmodium vivax* and *Plasmodium knowlesi* proteins involved in erythrocyte invasion. J. Exp. Med. 180, 497–506.

Coatney, G.R., Collins, W.E., Warren, M., Contacos, P.G., 1971. The Primate Malarias. U.S. Government Printing Office.

Conway, D.J., Cavanagh, D.R., Tanabe, K., Roper, C., Mikes, Z.S., Sakihama, N., Bojang, K.A., Oduola, A.M., Kremsner, P.G., Arnot, D.E., Greenwood, B.M., McBride, J.S., 2000. A principal target of human immunity to malaria identified by molecular population genetic and immunological analyses. Nat. Med. 6, 689–692.

Drakeley, C.J., Corran, P.H., Coleman, P.G., Tongren, J.E., McDonald, S.L., Carneiro, I., Malima, R., Lusingu, J., Manjurano, A., Nkya, W.M., Lemnge, M.M., Cox, J., Reyburn, H., Riley, E.M., 2005. Estimating medium- and long-term trends in malaria transmission by using serological markers of malaria exposure. Proc. Natl. Acad. Sci. U.S.A. 102, 5108–5113.

Escalante, A.A., Lal, A.A., Ayala, F.J., 1998. Genetic polymorphism and natural selection in the malaria parasite *Plasmodium falciparum*. Genetics 149, 189–202.

Escalante, A.A., Cornejo, O.E., Rojas, A., Udhayakumar, V., Lal, A.A., 2004. Assessing natural selection in malarial parasites. Trends. Parasitol. 20, 388–395.

Escalante, A.A., Cornejo, O.E., Freeland, D.E., Poe, A.C., Durrego, E., Collins, W.E., Lal, A.A., 2005. A monkey's tale: The origin of *Plasmodium vivax* as a human malaria parasite. Proc. Nat. Acad. Sci. U.S.A. 102, 1980–1985.

Espinosa, A.M., Sierra, A.Y., Barrero, C.A., Cepeda, L.A., Cantor, E.M., Lombo, T.B., Guzman, F., Avila, S.J., Patarroyo, M.A., 2003. Expression, polymorphism analysis, reticulocyte binding and serological reactivity of two *Plasmodium vivax* MSP-1 protein recombinant fragments. Vaccine 21, 1033–1043.

Fu, Y.X., Li, W.H., 1993. Statistical tests of neutrality of mutations. Genetics 133, 693–709.

Galinski, M.R., Medina, C.C., Ingravallo, P., Barnwell, J.W., 1992. A reticulocyte-binding protein complex of *Plasmodium vivax* merozoites. Cell 69, 1213–1226.

Good, M.F., Stanisic, D., Xu, H., Elliott, S., Wykes, M., 2004. The immunological challenge to developing a vaccine to the blood stages of malaria parasites. Immunol. Rev. 201, 254–267.

Hammer, M.F., Blackmer, F., Garrigan, D., Nachman, M.W., Wilder, J.A., 2003. Human population structure and its effects on sampling Y chromosome sequence variation. Genetics 164, 1495–1509.

Han, H.J., Park, S.G., Kim, S.H., Hwang, S.Y., Han, J., Traicoff, J., Kho, W.G., Chung, J.Y., 2004. Epidermal growth factor-like motifs 1 and 2 of *Plasmodium vivax* merozoite surface protein 1 are critical domains in erythrocyte invasion. Biochem. Biophys. Res. Commun. 320, 563–570.

Holder, A.A., Freeman, R.R., 1982. Biosynthesis and processing of a *Plasmodium falciparum* schizont antigen recognized by immune serum and a monoclonal antibody. J. Exp. Med. 156, 1528–1538.

Hudson, R.R., Kaplan, N.L., 1985. Statistical properties of the number of recombination events in the history of a sample of DNA sequences. Genetics 111, 147–164.

Hughes, A.L., 1992. Positive selection and intrallelic recombination at the merozoite surface antigen-1 (MSA-1) locus of *Plasmodium falciparum*. Mol. Biol. Evol. 9, 381–393.

Hughes, M.K., Hughes, A.L., 1995. Natural selection on *Plasmodium* surface proteins. Mol. Biochem. Parasitol. 71, 99–113.

John, C.C., O'Donnell, R.A., Sumba, P.O., Moormann, A.M., de Koning-Ward, T.F., King, C.L., Kazura, J.W., Crabb, B.S., 2004. Evidence that invasion-inhibitory antibodies specific for the 19 kDa fragment of merozoite surface protein-1 ($MSP\text{-}1_{19}$) can play a protective role against blood-stage *Plasmodium falciparum* infection in individuals in a malaria endemic area of Africa. J. Immunol. 173, 666–672.

Jongwutiwes, S., Tanabe, K., Nakazawa, S., Yanagi, T., Kanbara, H., 1992. Sequence variation in the tripeptide repeats and T cell epitopes in P190 (MSA-1) of *Plasmodium falciparum* from field isolates. Mol. Biochem. Parasitol. 51, 81–89.

Jongwutiwes, S., Tanabe, K., Kanbara, H., 1993. Sequence conservation in the C-terminal part of the precursor to the major merozoite surface proteins (MSP-1) of *Plasmodium falciparum* from field isolates. Mol. Biochem. Parasitol. 59, 95–100.

Joy, D.A., Feng, X., Mu, J., Furuya, T., Chotivanich, K., Krettli, A.U., Ho, M., Wang, A., White, N.J., Suh, E., Beerli, P., Su, X.Z., 2003. Early origin and recent expansion of *Plasmodium falciparum*. Science 300, 318–321.

Kaneko, O., Kimura, M., Kawamoto, F., Ferreira, M.U., Tanabe, K., 1997. *Plasmodium falciparum*: allelic variation in the merozoite surface protein 1 gene in wild isolates from southern Vietnam. Exp. Parasitol. 86, 45–57.

Kumar, S., Tamura, K., Jakobsen, I.B., Nei, M., 2001. MEGA2: molecular evolutionary genetics analysis software. Bioinformatics 17, 1244–1245.

Kumar, S.V., Ranjan, S., Saxena, V., Rajesh, V., Roy, S.K., Kochar, D., Ranjan, A., Das, A., 2005. *Plasmodium falciparum*: Genetic diversity of C-terminal region of MSP-1 in isolates from Indian sub-continent. Exp. Parasitol. 110, 384–388.

Li, W.H., 1993. Unbiased estimation of the rates of synonymous and non-synonymous substitution. J. Mol. Evol. 36, 96–99.

McDonald, J.H., Kreitman, M., 1991. Adaptive protein evolution at the Adh locus in *Drosophila*. Nature 351, 652–654.

Miller, L.H., Roberts, T., Shahabuddin, M., McCutchan, T., 1993. Analysis of sequence diversity in the *Plasmodium falciparum* merozoite surface protein-1 (MSP-1). Mol. Biochem. Parasitol. 59, 1–14.

Nei, M., Gojobori, T., 1986. Simple methods for estimating the numbers of synonymous and nonsynonymous nucleotide substitutions. Mol. Biol. Evol. 3, 418–426.

Nei, M., Kumar, S., 2000. Molecular Evolution and Phylogenetics. Oxford University Press.

O'Donnell, R.A., Saul, A., Cowman, A.F., Crabb, B.S., 2000. Functional conservation of the malaria vaccine antigen $MSP\text{-}1_{19}$ across distantly related Plasmodium species. Nat. Med. 6, 91–95.

Okech, B.A., Corran, P.H., Todd, J., Joynson-Hicks, A., Uthaipibull, C., Egwang, T.G., Holder, A.A., Riley, E.M., 2004. Fine specificity of serum antibodies to *Plasmodium falciparum* merozoite surface protein, PfMSP-1(19), predicts protection from malaria infection and high-density parasitemia. Infect. Immun. 72, 1557–1567.

Polley, S.D., Weedall, G.D., Thomas, A.W., Golightly, L.M., Conway, D.J., 2005. Orthologous gene sequences of merozoite surface protein 1 (MSP1) from *Plasmodium reichenowi* and *P. gallinaceum* confirm an ancient divergence of *P. falciparum* alleles. Mol. Biochem. Parasitol. 142, 25–31.

Putaporntip, C., Jongwutiwes, S., Seethamchai, S., Kanbara, H., Tanabe, K., 2000. Intragenic recombination in the 3′ portion of the merozoite surface protein 1 gene of *Plasmodium vivax*. Mol. Biochem. Parasitol. 109, 111–119.

Putaporntip, C., Jongwutiwes, S., Sakihama, N., Ferreira, M.U., Kho, W.G., Kaneko, A., Kanbara, H., Hattori, T., Tanabe, K., 2002. Mosaic organization and heterogeneity in frequency of allelic recombination of the *Plasmodium vivax* merozoite surface protein-1 locus. Proc. Natl. Acad. Sci. U.S.A. 99, 16348–16353.

Putaporntip, C., Jongwutiwes, S., Iwasaki, T., Kanbara, H., Hughes, A.L., 2006. Ancient common ancestry of the merozoite surface protein 1 of *Plasmodium vivax* as inferred from its homologue in *Plasmodium knowlesi*. Mol. Biochem. Parasitol. 146, 105–108.

Qari, S.H., Shi, Y.P., Goldman, I.F., Nahlen, B.L., Tibayrenc, M., Lal, A.A., 1998. Predicted and observed alleles of *Plasmodium falciparum* merozoite surface protein-1 (MSP-1), a potential malaria vaccine antigen. Mol. Biochem. Parasitol. 92, 241–252.

Rodríguez, L.E., Urquiza, M., Ocampo, M., Curtidor, H., Suarez, J., Garcia, J., Vera, R., Puentes, A., Lopez, R., Pinto, M., Rivera, Z., Patarroyo, M.E., 2002. *Plasmodium vivax* MSP-1 peptides have high specific binding activity to human reticulocytes. Vaccine 20, 1331–1339.

Rozas, J., Sanchez-DelBarrio, J.C., Messeguer, X., Rozas, R., 2003. DnaSP, DNA polymorphism analyses by the coalescent and other methods. Bioinformatics 19, 2496–2497.

Sachdeva, S., Ahmad, G., Malhotra, P., Mukherjee, P., Chauhan, V.S., 2004. Comparison of immunogenicities of recombinant *Plasmodium vivax* merozoite surface protein 1 19- and 42-kiloDalton fragments expressed in *Escherichia coli*. Infect. Immun. 72, 5775–5782.

Saitou, N., Nei, M., 1987. The Neighbor–Joining method: a new method for reconstructing phylogenetic trees. Mol. Biol. Evol. 4, 406–425.

Shi, Y.P., Sayed, U., Qari, S.H., Roberts, J.M., Udhayakumar, V., Oloo, A.J., Hawley, W.A., Kaslow, D.C., Nahlen, B.L., Lal, A.A., 1996. Natural immune response to the C-terminal 19-kilodalton domain of *Plasmodium falciparum* merozoite surface protein 1. Infect. Immun. 64, 2716–2723.

Snounou, G., White, N.J., 2004. The co-existence of *Plasmodium*: sidelights from *falciparum* and *vivax* malaria in Thailand. Trends Parasitol. 20, 333–339.

Stanisic, D.I., Martin, L.B., Gatton, M.L., Good, M.F., 2004. Inhibition of 19-kDa C-terminal region of merozoite surface protein-1-specific antibody responses in neonatal pups by maternally derived 19-kDa C-terminal region of merozoite surface protein-1-specific antibodies but not whole parasite-specific antibodies. J. Immunol. 172, 5570–5581.

Tajima, F., 1989. Statistical method for testing the neutral mutation hypothesis by DNA polymorphism. Genetics 123, 585–595.

Takala, S.L., Escalante, A.A., Branch, O.H., Kariuki, S., Biswas, S., Chaiyaroj, S.C., Lal, A.A., 2006. Genetic diversity in the Block 2 region of the merozoite surface protein 1 (MSP-1) of *Plasmodium falciparum*: additional complexity and selection and convergence in fragment size polymorphism. Infect. Genet. Evol. 6, 417–424.

Tanabe, K., Mackay, M., Goman, M., Scaife, J.G., 1987. Allelic dimorphism in a surface antigen gene of the malaria parasite *Plasmodium falciparum*. J. Mol. Biol. 195, 273–287.

Tanabe, K., Sakihama, N., Kaneko, A., 2004. Stable SNPs in malaria antigen genes in isolated populations. Science 303, 493.

Udhayakumar, V., Anyona, D., Kariuki, S., Shi, Y.P., Bloland, P.B., Branch, O.H., Weiss, W., Nahlen, B.L., Kaslow, D.C., Lal, A.A., 1995. Identification of T and B cell epitopes recognized by humans in the C-terminal 42-kDa domain of the *Plasmodium falciparum* merozoite surface protein (MSP)-1. J. Immunol. 154, 6022–6030.

Yang, C., Collins, W.E., Sullivan, J.S., Kaslow, D.C., Xiao, L., Lal, A.A., 1999. Partial protection against *Plasmodium vivax* blood-stage infection in Saimiri monkeys by immunization with a recombinant C-terminal fragment of merozoite surface protein 1 in block copolymer adjuvant. Infect. Immun. 67, 342–349.

International Immunology, Vol. 19, No. 3, pp. 311–320
doi:10.1093/intimm/dxl148

Type 1 cytokine/chemokine production by mouse NK cells following activation of their TLR/MyD88-mediated pathways

Junko Sawaki[1,2], Hiroko Tsutsui[3,4], Nobuki Hayashi[2,4], Koubun Yasuda[2,4], Shizuo Akira[5], Takakuni Tanizawa[1] and **Kenji Nakanishi[2,4]**

[1]Department of Pediatrics
[2]Department of Immunology and Medical Zoology and
[3]Department of Microbiology, Hyogo College of Medicine, 1-1, Mukogawa-cho, Nishinomiya 663-8501, Japan
[4]Core Research of Evolutional Science and Technology, Japan Science and Technology Agency, Kawaguchi 332-0012, Japan
[5]Department of Host defenses, Research Institute for Microbial Diseases, Osaka University, Osaka 565-0871, Japan

Keywords: CCL3, CCL4, IFN-γ, IL-12, NK lytic activity

Abstract

It is well established that IL-18R- and toll-like receptor (TLR)-mediated signalings share a common signal pathway mediated by signal adaptor, MyD88, and that IL-18 synergizes with IL-12 for IFN-γ production by NK cells. Here, we investigated whether TLR agonists can replace IL-18 for production of IFN-γ by NK cells. Freshly isolated NK cells possessed functional LPS receptor composed of TLR4/MD2 complex and of CD14, and also expressed other various *tlrs*. Hepatic $CD3^{-}DX5^{+}$ NK cells produced IFN-γ in response to TLR2 or TLR7 agonists only when co-stimulated with IL-12, indicating that TLR agonists synergize with IL-12 for IFN-γ. The $tlr2^{-/-}$ or $tlr7^{-/-}$ NK cells could not produce IFN-γ in response to IL-12 plus TLR2 or TLR7 ligands, respectively, indicating requirement of the corresponding TLRs. Furthermore, upon stimulation with these combinations, wild-type NK cells produced type 1 chemokines, such as CCL3, CCL4 and CCL5 as well. NK cells from bacterium (e.g. *Propionibacterium acnes*)-inoculated $rag2^{-/-}$ mice, when compared with those from naive mice, exhibited significantly enhanced capacity to produce these CC chemokines and IFN-γ, suggesting that microbial infection enhances responsiveness of NK cells to TLR agonists. These results indicate that upon microbial infection, macrophages produce IL-12 that renders NK cells highly responsive to TLR agonists to produce IFN-γ and chemokines, which might in turn recruit and fully activate macrophages, leading to the development of inflammatory foci presumably necessary for efficient microbial eradication. Thus, NK cells, like T cells, induce orchestrated immune responses in collaboration with macrophages to show potent host defense effects during early infectious phase.

Introduction

NK cell is an important constituent of innate immunity that plays an essential role in host defense, particularly at early infectious phases (1, 2). Indeed, mice genetically lacking T cells and B cells, such as SCID or $rag1^{-/-}$ mice, can eradicate pathological microbes in an IFN-γ- and NK cell-dependent manner (3, 4). It is well established that upon infection of mice with *Listeria monocytogenes*, a facultative gram-positive intracellular bacterium, dendritic cells (DCs) and macrophages produce IFN-γ-inducing cytokines, such as IL-12 and IL-18, via activation of their toll-like receptor (TLR)/MyD88-mediated signal pathways, important innate immune signalings (5–7). IL-18 can activate NK cells to produce robust IFN-γ in combination with other IFN-γ-inducing cytokine such as IL-12 (8–10). This IFN-γ, in turn, activates macrophages to accomplish their listeriocidal actions during the early infectious phase, eventually resulting in the early listerial clearance (1, 2). Indeed, the depletion of NK cells or IFN-γ gene renders mice highly vulnerable to *L. monocytogenes*. As previously reported, $il18^{-/-}$ mice are susceptible to *L. monocytogenes* due to the impaired induction of IFN-γ (5). Intriguingly, $il12^{-/-}$ mice are as vulnerable as $ifng^{-/-}$, but much more susceptible than $il18^{-/-}$ mice, allowing us to propose the possibility that some factors other than IL-18 might cooperate with endogenous IL-12 for the NK cell production of IFN-γ.

Correspondence to: K. Nakanishi; E-mail: nakaken@hyo-med.ac.jp

Transmitting editor: T. Hamaoka

Received 23 October 2006, *accepted* 22 December 2006

Advance Access publication 7 February 2007

We now know that the TLR-mediated pathways share a signal cascade with IL-18 signaling (6, 7, 11, 12). Both IL-18 and TLR ligands require MyD88, a signal adaptor, to activate NF-κB. Therefore, it is plausible that TLR agonists can replace IL-18 and synergize with IL-12 for IFN-γ production by NK cells. Furthermore, in analog with IL-18 induction of chemokines (13, 14) by macrophages, TLR agonists seem to induce chemokine production by NK cells (6). In this study, we addressed these questions and found that murine NK cells constitutively express functional TLRs and produce IFN-γ in response to TLR ligands, like to IL-18 in the presence of IL-12 in a corresponding TLR- and MyD88-dependent manner. Furthermore, the NK cells simultaneously produced robust CC chemokines, CCL3, CCL4 and CCL5, which can recruit various subtypes of leukocytes including macrophages (15). Finally, we assessed physiological roles of the TLR-mediated NK cell activation. Naive NK cells produced little or a small amount of those chemokines upon stimulation with TLR agonists without IL-12. By contrast, bacterium-elicited NK cells were well armed and capable of producing much larger amounts of the chemokines, indicating that microbial infection commits NK cells competent to directly respond to TLR ligands. These results provide new insights into NK cell responses early in infection.

Methods

Mice

C57BL/6 mice were purchased from Crea Japan (Osaka, Japan). *rag2*$^{-/-}$ mice were purchased from Jackson Laboratory (Bar Harbor, ME, USA). *tlr2*$^{-/-}$ mice (16), *tlr7*$^{-/-}$ mice (17) and *myd88*$^{-/-}$ mice (11) were backcrossed with C57BL/6 mice, and F8 to F10 generations were used. The *il12*$^{-/-}$ *il18*$^{-/-}$ mice were shown elsewhere (5). All mice were kept under SPF conditions and received humane care as outlined in the Guide for the Care and Use of Experimental Animals (Hyogo Medical College Animal Care Committee).

Reagents

LPS derived from *Escherichia coli* O11:B5 was purchased from Sigma (St Louis, MO, USA). TLR2 agonist, peptidoglycan (PGN), and TLR3 agonist, poly (I):poly (C), were from Fluka (Bachs, Sweden) and Amersham Pharmacia Biotech (Freiburg, Germany), respectively. TLR7 agonist, Loxoribine (18), was purchased from InvivoGen (San Diego, CA, USA). Anti-DX5-bound microbeads and anti-FITC-bound microbeads were purchased from Miltenyi Biotec Inc. (Auburn, CA, USA). Recombinant mice IL-12 and IL-18 were obtained from R&D (Minneapolis, MN, USA) and MBL (Nagoya, Japan), respectively. Recombinant human IL-15 was from Peprotech (London, UK). Recombinant human IL-2 was kindly provided by Shionogi Pharmaceuticals (Osaka, Japan). FITC-conjugated anti-CD3 and PE-conjugated DX5 were purchased from PharMingen (San Diego, CA, USA). FITC-conjugated anti-TLR4-MD2 complex was kindly provided by Dr. K. Miyake at the University of Tokyo (Tokyo, Japan). *Propionibacterium acnes* were killed at 60°C for 4 h as previously shown (19). RAW264.7, mouse macrophage cell line, was used (20). The culture medium generally used in this study is RPMI 1640 containing 10% FCS, 100 U ml^{-1} penicillin, 100 μg ml^{-1} streptomycin, 50 μM of 2-ME and 2 mM L-glutamine.

Preparation of NK cells

CD3$^-$DX5$^+$ cells were prepared by using autoMACS (Miltenyi Biotec Inc.) as described before (21, 22) or were sorted by FACSaria (Becton Dickinson, Mountain View, CA, USA). Hepatic CD3$^-$DX5$^+$ cells prepared from *P. acnes*-primed mice (19) were incubated with 300 ng ml^{-1} of rIL-15 for 10 days and used as IL-15-expanded NK cells. The purity of CD3$^-$DX5$^+$ cells expanded was >85%. Splenic DX5$^+$ cells were also prepared from *rag2*$^{-/-}$ treated with or without *P. acnes* using autoMACS. The cells were incubated with PGN (100 and 10 μg ml^{-1}), poly I:C (100 and 10 μg ml^{-1}) or loxoribine (1000 and 100 nM) in the presence of various recombinant cytokines for 48 h, and supernatants were collected.

Assay for cytokines and chemokines

Concentrations of IFN-γ, IL-13, tumor necrosis factor (TNF)-α, CCL3, CCL4 and CCL5 in each supernatant were measured by a commercially available kit (R&D).

FACS

Cells were incubated with PE-conjugated anti-DX5, Allophycocyanin-conjugated anti-CD3 and FITC-conjugated anti-TLR4-MD2 complex or anti-CD14 after FcR blocking (22). Stained cells were analyzed using FACScalibur (Becton Dickinson) (23).

Assay for NK lysis

IL-15-expanded hepatic CD3$^-$DX5$^+$ cells were incubated with PGN (100 μg ml^{-1}), poly I:C (100 μg ml^{-1}) or loxoribine (1 μM) in the presence of IL-12 (200 pg ml^{-1}) for 24 h. NK lytic activity against YAC-1 cells was determined by the method described previously (24).

EMSA

Double-stranded, NF-κB-specific oligonucleotide, the consensus sequence (5′-TCG-AGG-GCT-GGG-GAT-TCC-CCA-TCT-C-3′), was labeled with [^{32}P] dCTP and used as probe. Cells were incubated with 1 μg of LPS or 10 ng of IL-18 for the indicated hours, and nuclear localization of NF-κB was determined by using the cell extract as previously described (25). Briefly, nuclear extracts (20 μg) were incubated with the probe and electrophoresed, and gel was subsequently dried and visualized by autoradiography.

Reverse transcription–PCR

Total RNA was extracted, and mRNA for TLR1, 2, 3, 4, 5, 6, 7, 9 and β-actin was determined by reverse transcription–PCR (25). The individual primers and amplifying cycle were shown in Table 1.

Statistics

All data are shown as the mean ± SD of triplicate samples. Significance between the experimental and control groups was examined by the unpaired Student's *t*-test.

Table 1. Reverse transcription–PCR for murine TLRs

	Sense primer	Anti-sense primer	Cycle
tlr1	tct ctg aag gct ttg tcg ata ca	gac aga gcc tgt aag cat att cg	35
tlr2	tct aaa gtc gat ccg cga cat	tac cca gct cgc tca cta cgt	35
tlr3	ttg tct tct gca cga acc tg	cgc aac gca agg att tta tt	35
tlr4	caa gaa cat aga tct gag ctt caa cc	gct gtc caa tag gga agc ttt cta ga	35
tlr5	act gaa ttc ctt aag cga cgt a	aga aga taa agc cgt gcg aaa	35
tlr6	aac agg ata cgg agc ctt ga	cca gga aag tca gct tcg tc	35
tlr7	ttc cga tac gat gaa tat gca cg	tga gtt tgt cca gaa gcc gta at	35
tlr8	ggc aca act ccc ttg tga tt	cat ttg ggt gct gtt gtt tg	35
tlr9	ccg caa gac tct att tgt gct gg	tgt ccc tag tca ggg ctg tac tca g	35
β-actin	gat gac gat atc gct gcg ctg	gta cga cca gag gca tac agg	28

Results

NF-κB activation in response to LPS

First, we investigated NK cell expression of TLRs. Hepatic $CD3^-DX5^+$ cells freshly isolated from naive wild-type (WT) mice expressed *tlr1*, *tlr2*, *tlr3*, *tlr4*, *tlr6*, *tlr7*, *tlr8* and *tlr9* (Fig. 1A). This was also the case for splenic NK cells (data not shown). These results indicate that mouse NK cells express various TLRs under normal conditions. As both TLR4/MD2 complex and CD14 are required for the TLR4-mediated signal pathway (26, 27), we analyzed their expressions of these molecules. FACS-sorted hepatic $CD3^-DX5^+$ NK cells moderately expressed these receptors on their surface (Fig. 1B). The cells incubated with control mAbs showed the same intensity for those molecules as the backgrounds (data not shown). NK cells expressed less amounts of TLR4/MD2 complex than RAW cells, mouse macrophage cell line (Fig. 1B).

As NF-κB activation is a hallmark of the TLR-mediated signalings (6, 9, 10, 28), we examined whether NK cells show the DNA-binding activity of NF-κB promptly after stimulation with LPS, TLR4 agonist. Because freshly isolated NK cells showed too low yield to examine further, we expanded them with IL-15 (29). The IL-15-expanded cells still had $CD3^-DX5^+$ cells at >85% (Fig. 1B). The IL-15-expanded hepatic NK cells expressed various *tlrs* except for *tlr5* and *tlr8* (Fig. 1A) and TLR4/MD2 and CD14 on their surface as well (Fig. 1B). Thus, we used IL-15-expanded cells thereafter to examine NK cell potential via activating their TLRs. Like IL-18, LPS could induce nuclear NF-κB accumulation in NK cells (Fig. 1C). These results indicated that the IL-15-expanded hepatic NK cells are able to respond to LPS at least in terms of NF-κB activation without help from other cell types. This was also true for splenic NK cells (data not shown). These results suggested that NK cells as well as macrophages and DCs might be able to sense TLR ligands.

Synergistic action of TLR agonists with IL-12 for IFN-γ production

Next, we wanted to know biological products of TLR agonist-activated NK cells. As IL-18 is a potent IFN-γ-inducing cytokine, we focused on the action of TLR agonists on IFN-γ production by NK cells. We prepared hepatic NK cells expanded with IL-15 for 10 days and incubated them with various TLR agonists. PGN (TLR2), poly I:C (TLR3) or loxoribine (TLR7) stimulation solely could not induce IFN-γ (Fig. 2). This was also the case for NK cells expanded with IL-15 for 6 days (Supplementary Figure 1, available at *International Immunology* Online). However, the TLR agonists synergized with IL-12 for induction of production of IFN-γ (Fig. 2), which is similar to the synergism between IL-18 and IL-12 (9, 30, 31). Although IL-18 shows somewhat synergy with IL-2 or IL-15 (9), TLR agonists did not synergize with these cytokines for IFN-γ production by NK cells (Fig. 2). Since NK cells can produce TNF-α or IL-13 (9), we examined whether TLR agonists, in combination with IL-12 or solely, induce these cytokines in NK cells. The cells produced little IL-13 and TNF-α (Fig. 3). Intriguingly, they could not produce TNF-α (Fig. 3) or IL-6 (data not shown), strongly suggesting that the NK cell preparation seems not to be contaminated with the cells that produce TNF-α and/or IL-6 in response to the TLR agonist, such as macrophages and DCs. We next tested whether IL-12 dose dependently induce IFN-γ when in conjunction with TLR ligands. Expectedly, we found the dose dependency (Fig. 4A). This does not exclude the possibility that TLR-expressing macrophages are contaminated in the NK cell preparation and produce IL-18 in response to TLR agonists, which eventually induce IFN-γ in collaboration with exogenous IL-12. To neglect this possibility, we stimulated NK cells prepared from $il12^{-/-}$ $il18^{-/-}$ mice with the TLR agonists plus IL-12 and found their production of IFN-γ (Fig. 4B). Those characteristics were also found in IL-15-expanded splenic NK cells (data not shown). These results indicated that NK cells have potential to respond to TLR agonists in the presence of IL-12 by production of IFN-γ.

Requirement of corresponding TLRs and MyD88 for the IFN-γ production

We next investigated whether TLR agonists/IL-12-induced IFN-γ requires the corresponding TLRs. We manipulated hepatic $CD3^-DX5^+$ NK cells prepared from WT, $tlr2^{-/-}$ and $tlr7^{-/-}$ mice. The $tlr2^{-/-}$ NK cells produced IFN-γ in response to poly I:C and loxoribine, but not PGN (Fig. 5), indicating requirement of TLR2 for PGN induction of IFN-γ. The $tlr7^{-/-}$ cells produced IFN-γ in response to poly I:C and PGN, but not loxoribine (Fig. 5), indicating requirement of TLR7 for loxoribine induction of IFN-γ. Therefore, corresponding TLRs are essential.

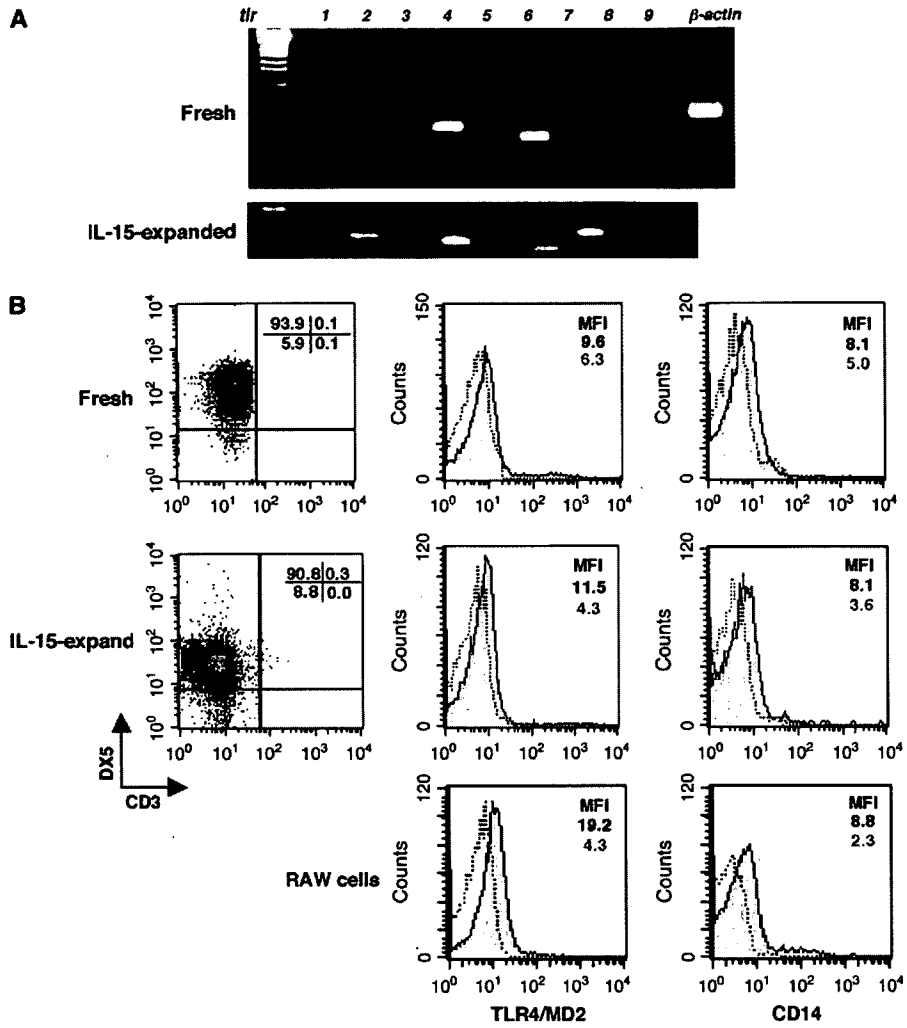
A
tlr
1
2
3
4
5
6
7
8
9
β-actin
Fresh
IL-15-expanded
B
Fresh
IL-15-expand
RAW cells
93.9 0.1
5.9 0.1
90.8 0.3
8.8 0.0
DX5
CD3
Counts
MFI
9.6
6.3
MFI
8.1
5.0
MFI
11.5
4.3
MFI
8.1
3.6
MFI
19.2
4.3
MFI
8.8
2.3
TLR4/MD2
CD14
C
Post stimulation (min)
LPS
IL-18
0
15
30
45
60
60
NF-κB

Next, we examined whether MyD88 (6) is required for these IFN-γ production. As expected, *myd88*$^{-/-}$ cells exhibited little increase in production of IFN-γ in response to the TLR2/7 agonists in the presence of IL12 (Fig. 5), demonstrating that the TLR2- and TLR7-mediated IFN-γ production by NK cells requires MyD88. Consistent with the previous reports (6, 7), MyD88 is dispensable for TLR3-mediated IFN-γ production (Fig. 5). Those characteristics were also true for IL-15-expanded splenic NK cells (data not shown). Collectively, NK cells have potential to produce IFN-γ via activation of their corresponding TLRs and MyD88.

Lack of up-regulating action of TLR agonists onto NK lytic activity

Since IL-18 up-regulates NK lytic activity, we next examined effects of the TLR agonists. NK cells did not show increased lytic activity against YAC-1 cells, authentic murine NK target cells, after stimulation with the agonists either in the presence or in the absence of IL-12 (Fig. 6). Thus, NK killing activity is not profoundly affected by the treatment with TLR agonists.

Type 1 chemokine productions

It has been demonstrated that NK cells become to cytoplasmically possess CCL3 (MIP-1α), CCL4 (MIP-1β) and CCL5 (RANTES) *in vivo* after infection of mice (32–34) but the mechanism underlying is still to be elucidated. Thus, we assumed that microbial TLR agonists directly activate NK cells under influence of IL-12. We measured those chemokine levels in the supernatants of NK cells stimulated with TLR agonists *in vitro*. CD3$^-$DX5$^+$ NK cells produced CCL3, CCL4 and CCL5 in response to the TLR2, TLR3 and TLR7 agonists plus IL-12 (Fig. 7). Those characteristics were also found by using IL-15-expanded splenic NK cells (data not shown). Separately, we observed that IL-15-expanded NK cells could produce IFN-γ and CCL3 in response to TLR4 and TLR9 ligands in the presence of IL-12 (Supplementary Figure 2, available at *International Immunology* Online), indicating

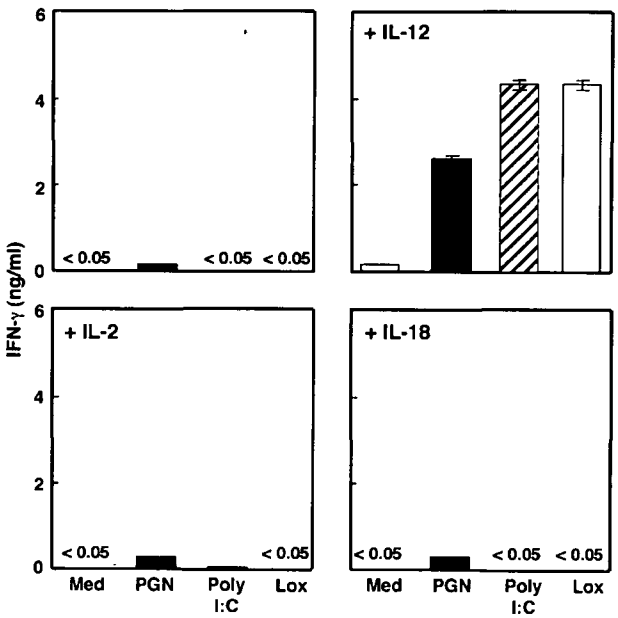

Fig. 2. IL-12, but not IL-2 or IL-18, synergizes with TLR agonists for IFN-γ by NK cells. IL-15-expanded NK cells were incubated with PGN (100 μg ml^{-1}), poly I:C (100 μg ml^{-1}) or loxoribine (Lox, 1000 μM) in the presence or absence of IL-12 (2000 pg ml^{-1}), IL-2 (500 U ml^{-1}) or IL-18 (10 ng ml^{-1}) for 48 h. IFN-γ in each supernatant was measured by ELISA. The data are expressed as mean ± SD of triplicates. The data are representative of three independent experiments with the similar results.

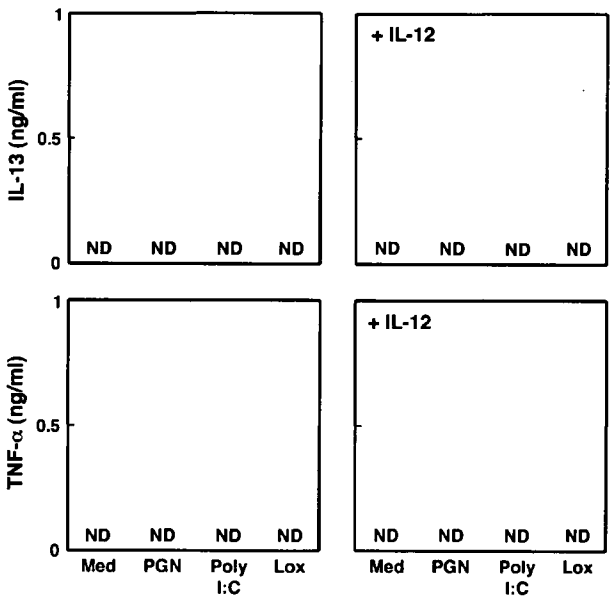

Fig. 3. NK cells do not produce IL-13 or TNF-α in response to IL-12 plus TLR agonists. IL-15-expanded hepatic NK cells were incubated with the TLR agonists shown in the legend to Fig. 2 in the presence of IL-12 (2000 pg ml^{-1}) for 48 h. IL-13 and TNF-α concentrations in each supernatant was measured. ND indicates that concentrations of IL-13 and TNF-α are <0.01 ng ml^{-1}. The data are expressed as mean ± SD and representative of three independent experiments with the similar results.

Fig. 1. Constitutive expressions of *tlrs* in NK cells. (A) Total RNA was extracted from freshly isolated, FACS-sorted hepatic CD3$^-$DX5$^+$ cells (fresh) or the cells that were expanded from the same cell fraction with IL-15 for 10 days (IL-15-expanded), and reverse transcription–PCR was performed for various TLRs by using corresponding primers. (B) Purity of CD3$^-$DX5$^+$ cells in 'fresh' and 'IL-15-expanded' was determined. Insets indicate cell percentage of each quadrant. fresh, IL-15-expanded cells and RAW cells were incubated with anti-TLR4/MD2 complex or anti-CD14 mAmAb (solid lines). Dotted lines indicate background staining. (C) IL-15-expanded hepatic CD3$^-$DX5$^+$ NK cells were incubated with LPS (100 ng ml^{-1}) or IL-18 (10 ng ml^{-1}) for the indicated periods. Nuclear proteins were extracted, and EMSA for NF-κB was performed. Representative photographs were shown (A). The data are representative of three independent experiments with the similar results.

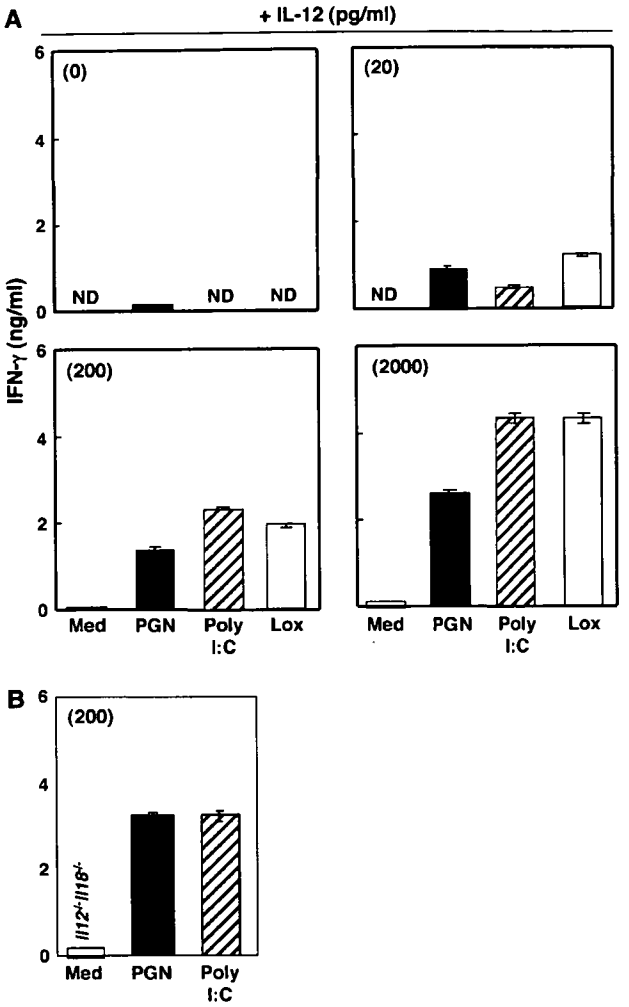

Fig. 4. IL-12 dose dependently induces IFN-γ in collaboration with various TLRs. IL-15-expanded hepatic NK cells were incubated with the TLR ligands shown in the legend to Fig. 2 in the presence of various doses of IL-12. IFN-γ concentration in each supernatant was measured. The data are expressed as mean ± SD and representative of three independent experiments with the similar results.

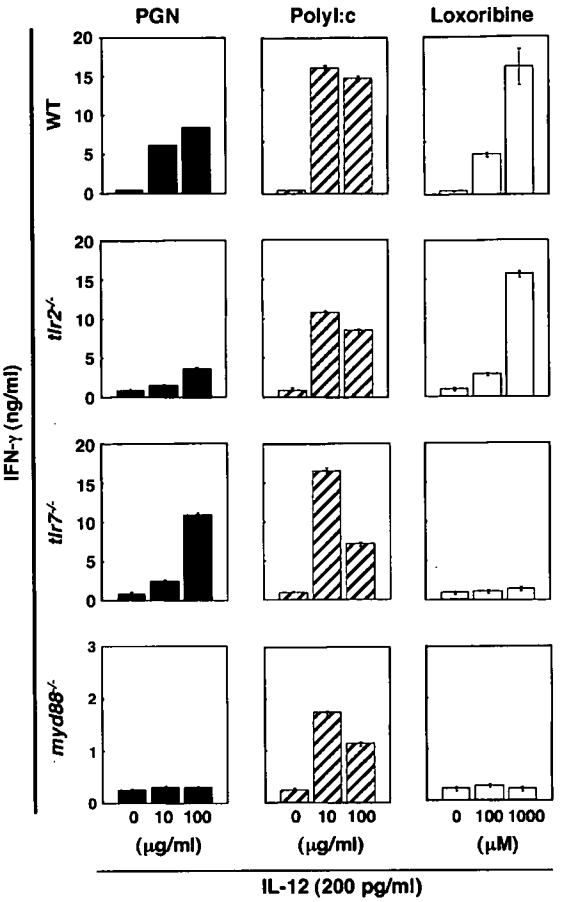

Fig. 5. TLR- and MyD88-dependent IFN-γ production. IL-15-expanded hepatic NK cells were prepared from WT, *tlr2*$^{-/-}$, *tlr7*$^{-/-}$ or *myd88*$^{-/-}$ mice and incubated with the various doses of TLR agonists in the presence of IL-12 for 48 h. IFN-γ concentration in each supernatant was measured. The data are expressed as mean ± SD and representative of three independent experiments with the similar results.

TLR4- and TLR9-mediated activation of NK cells for production of type 1 cytokine/chemokine. These results indicated again that TLR agonists synergize with IL-12 for induction of production of the chemokines by NK cells.

Enhancement of TLR-mediated NK cell responses by in vivo administration of heat-killed bacterium

All the results indicate that NK cells have potential to respond to various TLR agonists by producing type 1 cytokine/chemokines. These results led us to know physiological roles of the TLR-mediated activation of NK cells. To address this, we investigated whether microbial infection enhances this NK cell response particularly in the innate immune phase. To exclude the possible interference with harmful exotoxins and/or enzymes produced by live bacterium and evaluate responses only to the bacterial components, we systemically administered heat-killed *P. acnes*, a gram-positive bacterium, into *rag2*$^{-/-}$ mice and compared responses of their NK cells with PGN, TLR agonists of gram-positive bacteria, with those in naive mice. NK cell purity of the MACS-sorted DX5^{+} cells prepared from naive and *P. acnes*-primed *rag2*$^{-/-}$ mice were 96 and 94%, respectively (Fig. 8A). As compared with naive cells, *P. acnes*-elicited NK cells produced five to 10 times more amounts of CCL3 and CCL4 in response to PGN (Fig. 8B), indicating that *in vivo* treatment with *P. acnes* renders NK cells more sensitive to PGN. However, either *P. acnes*-elicited or naive NK cells did not produce IFN-γ in response to PGN in the absence of IL-12 (Fig. 8B). Intriguingly, in the presence of IL-12, the former cells turned to produce IFN-γ at larger amounts (Fig. 8C), indicating that *P. acnes*-elicited NK cells still require IL-12 for production of IFN-γ and again augmenting effects of *P. acnes* treatment on the TLR-mediated IFN-γ production from NK cells. These results indicated that infected macrophages augment their anti-microbial functions

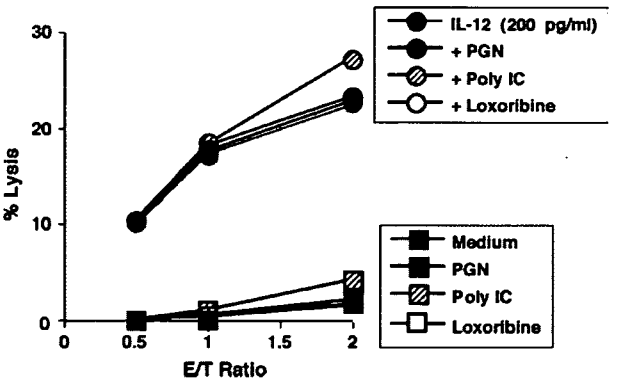

Fig. 6. Lack of enhancing effects of TLR agonists on NK cytolytic activity. IL-15-expanded hepatic NK cells were incubated with various TLR ligands in the presence or absence of IL-12. Their cytotoxicity against YAC-1 cells was evaluated. The data are expressed as mean and representative of three independent experiments with the similar results.

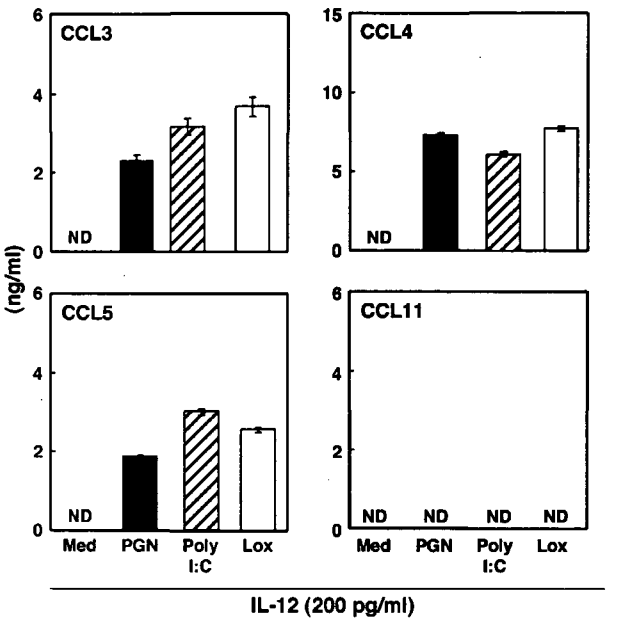

Fig. 7. NK cell production of CCL3, CCL4 and CCL5 in response to IL-12 plus TLR agonists. IL-15-expanded hepatic NK cells were incubated with the various TLR agonists shown in Fig. 2 in the presence of IL-12 for 48 h. CCL3, CCL4, CCL5 and CCL11 in each supernatant were measured. The data are expressed as mean ± SD and representative of three independent experiments with the similar results.

by arming NK cells with enhanced production of IFN-γ and chemokines upon TLR agonist challenge, that in combination induces strong innate immune responses.

Discussion

In this study, we demonstrated that NK cells are activated through their TLRs for production of IFN-γ, CCL3, CCL4 and CCL5, which are essential for efficient microbial clearance. Various TLR agonists could activate NK cells to produce those type 1 cytokine/chemokines in synergy with IL-12, but not with IL-18 or IL-2, and these responses depended on the corresponding TLRs and MyD88 (Figs 4, 5 and 7). Importantly, these actions were extensively enhanced by the treatment of mice with heat-killed *P. acnes* (Fig. 8). Indeed, *P. acnes*-elicited NK cells produced much larger amounts of those CC chemokines upon stimulation with *P. acnes*-derived TLR agonist, PGN, than naive cells (Fig. 8). These results suggested that microbial infection of mice induces NK cells to become competent to directly respond to the microbial TLR ligands. Based on these observations, one can imagine the following scenario for the early microbial eradication. Following microbial infection, tissue macrophages and DCs produce IL-12 in response to the microbial TLR ligands, and IL-12-stimulated NK cells become highly susceptible to these ligands. Therefore, there is positive feedback between TLR-mediated IL-12 and TLR ligand responsiveness of IL-12-stimulated NK cells. After recognizing the microbial TLR ligands, the NK cells in the infectious sites produce robust CCL3, CCL4 and CCL5, which eventually induces migration of TLR-expressing macrophages around the NK cells in the infectious sites. These migrated macrophages recognize the microbial TLR ligands of the infectious sites and increase production of IL-12 and other IFN-γ-inducing cytokines, which eventually and fully activate the NK cells to further produce IFN-γ. Furthermore, IL-12-stimulated NK cells increase production of IFN-γ and chemokines in response to the microbial TLR agonists at the infected sites. Thus, IFN-γ production from NK cells is positively regulated by TLR agonists and IL-12. These events might converge into the histological formation of inflammatory foci around the microbe and the generation of a powerful positive circuit between NK cells and macrophages, leading to the efficient early host defense. It is noted that IL-12 is solely capable of activating naive and *P. acnes*-elicited NK cells to produce IFN-γ (Fig. 8), but poorly the chemokines (data not shown), indicating that IL-12 by itself cannot activate the positive circuit. Convincingly, microbial infection renders NK cells competent to the microbial TLR agonists via induction of DC or macrophage IL-12 production.

The mechanism underlying the increased responsiveness of NK cells to TLR agonists during *P. acnes* treatment is still to be elucidated. To investigate possible involvement of IFN-γ in this response, we administered neutralizing anti-IFN-γ into mice on and after *P. acnes* treatment. However, IFN-γ blockade did not reduce their responsiveness to PGN (data not shown), indicating minor role of endogenous IFN-γ in the facilitated responsiveness of NK cells to TLR agonists. We need further study to conclude that endogenous IL-12 contributes to this differentiation of NK cells.

It has been reported that various chemokines and their receptors contribute to host defense. In particular, CCR5 and its ligands, CCL3, CCL4 and CCL5, are important. The *ccl3*$^{-/-}$ mice have defects in protection against viral infection with concomitant numerical reduction of infiltrated NK cells and abolition of elevated IFN-γ in the infection sites (32, 35), indicating the importance of CCL3 for the recruitment of IFN-γ-producing NK cells and presumably of

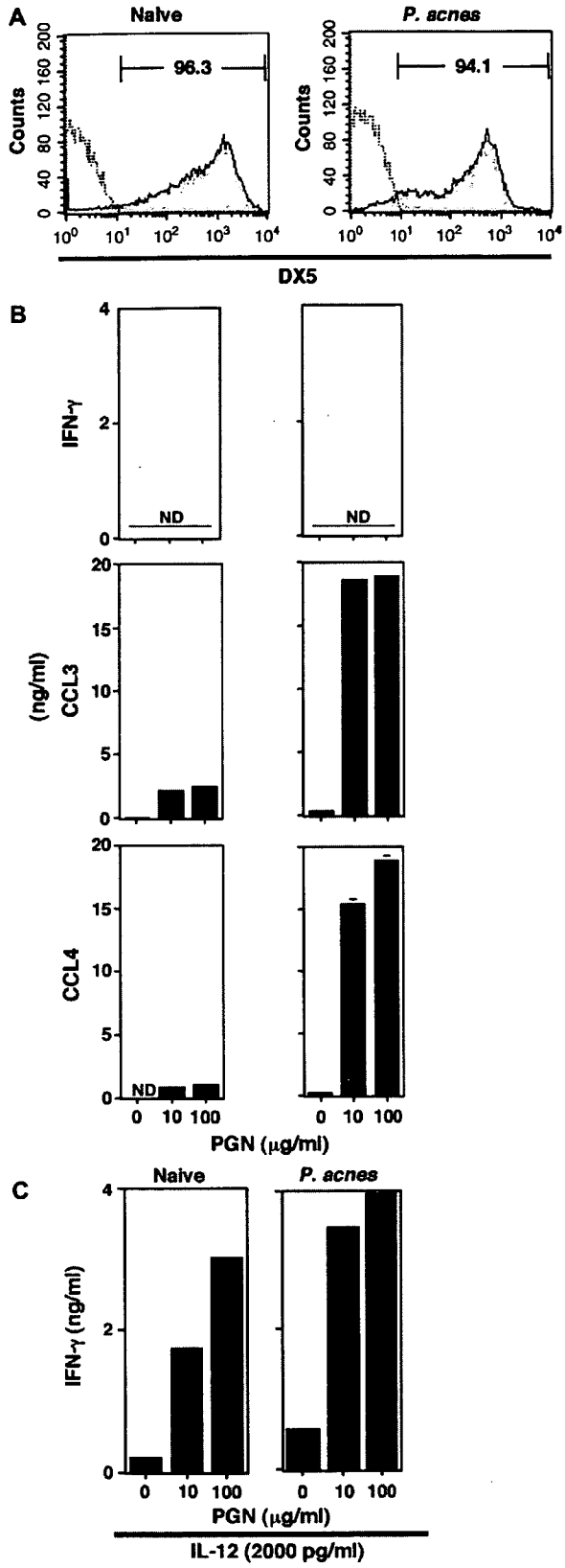

IL-12-producing DCs and macrophages. Indeed, DCs and macrophages as well as NK cells express CCR5 (15, 36, 37). Expectedly, mice deficient in CCR5, like *ccl3*$^{-/-}$ mice, are highly susceptible to infection with intracellular pathogenic fungi and various viruses (37, 38). It was previously reported that following viral infection, NK cells produce CCL3 and CCL4 via activation of their activating receptors and/or in response to endogenous type I IFN (34, 39, 40). Our present results clearly demonstrate a third chemokine-inducing tool equipped by NK cells. NK cells produce those CCR5 ligands in response to TLR agonists (Fig. 8). Therefore, it is convincing that the TLR/MyD88-mediated NK cell production of these chemokines might also contribute to the eradication of various types of microbes.

Synergy of IL-18 and IL-12 for IFN-γ is partly attributed to the up-regulated expression of IL-18R by IL-12R and vice versa (9, 29). In analog with this, we investigated whether TLR expressions on NK cells are also increased after stimulation with IL-12. However, IL-12 did not induce increase of TLR4/MD2 or CD14 expressions in NK cells (data not shown). It was shown that the synergy occurs at the signaling levels via activation of both NF-κB and stat4, which are induced by IL-18 and IL-12, respectively (9, 41). TLR ligands, like IL-18, can activate NF-κB as well (Fig. 1C). Therefore, synergistic action of TLR agonists and IL-12 for their IFN-γ might be regulated at their signaling levels similar to that of IL-18 and IL-12 (9, 41).

TLR ligands, unlike IL-18, did not augment murine NK cytotoxicity even in the presence of IL-12 (Fig. 6). As previously reported, murine NK cells show increased perforin- or Fas ligand-dependent NK lytic activities after stimulation with IL-18 (24, 42). IL-12, like IL-18, up-regulates perforin-dependent NK activity both *in vitro* (24). However, unlike for IFN-γ production, these two cytokines do not synergize for increase of NK cytolitic activity (24). Furthermore, IL-18 can augment NK lytic activity in the absence of IL-12 (24), strongly indicating that IL-18 signaling for up-regulating NK cell killing activity might be independent of that for IFN-γ production (9, 41). Accordingly, TLR ligands can replace IL-18 for IFN-γ production presumably via activation of NF-κB, but not activate the signal pathway for NK cytolysis induced by IL-18. Further study is required for the identification of this signal pathway of IL-18 up-regulation of NK lysis, that is not shared by the TLR-mediated signal pathway. Importantly, in contrast to our results of mouse NK cells, human NK cells show increased NK lytic activity upon stimulation with TLR agonists (43–46). We need further study to clarify the molecular mechanisms differentially underlying those two species.

There is a possibility that IL-15-expanded $CD3^{-}DX5^{+}$ population is contaminated with non-NK cells that might produce the upstream cytokines that might induce type 1

Fig. 8 *Propionibacterium acnes* treatment induces responsiveness of NK cells to TLRs agonists. NK cells freshly isolated from naive or *P. acnes*-primed mice were stained with anti-DX5 and anti-CD3 for determination of NK cell purity (A). The cells were incubated with PGN in the presence (C) or absence (B) of IL-12 for 48 h. IFN-γ, CCL3 and CCL4 concentrations in each supernatant were measured. The data are expressed as mean ± SD and representative of three independent experiments with the similar results.

cytokine/chemokine production from NK cells. To exclude this possibility, we used mouse-cloned NK cells, namely, LNK5E6 cells and analyzed their potentials (42). The LNK cells similarly expressed various TLRs as in freshly isolated and IL-15-expanded NK cells (Supplementary Figure 3, available at *International Immunology* Online). Furthermore, the cells synergistically produced IFN-γ in response to TLR7 ligands and IL-12. These results support our conclusion that NK cells are directly activated through their TLRs for production of type 1 cytokine/chemokine, which may eventually lead to the early microbial clearance.

In summary, our present results clearly showed that NK cells produce robust IFN-γ and CCR5 ligands in response to TLRs plus IL-12 and suggested that the NK cells activated by this combination might be essential for the efficient early eradication of pathogenic microbes. Although we need further studies to evaluate *in vivo* precise roles of these NK cell responses, our present observations still provide new insights into NK cell activation in the host defense, particularly at the early infectious phase.

Supplementary data

Supplementary figures 1, 2 and 3 are available at *International Immunology* Online.

Acknowledgements

This study was partly supported by Grants and a Hitec Research Center Grant from the Ministry of Education, Culture, Sports, Science and Technology of Japan. We thank Ms Shizue Yumikura-Futatsugi and Ms Noriko Nakano for excellent technical assistance.

Abbreviations

DC	dendritic cell
PGN	peptidoglycan
TLR	toll-like receptor
TNF	tumor necrosis factor
WT	wild type

References

1 Biron, C. A., Nguyen, K. B., Pien, G. C., Cousens, L. P. and Salazar-Mather, T. P. 1999. Natural killer cells in antiviral defense: function and regulation by innate cytokines. *Annu. Rev. Immunol.* 17:189.
2 Lanier, L. L. 2005. NK cell recognition. *Annu. Rev. Immunol.* 23:225.
3 Unanue, E. R. 1997. Inter-relationship among macrophages, natural killer cells and neutrophils in early stages of *Listeria* resistance. *Curr. Opin. Immunol.* 9:35.
4 Kaufmann, S. H.E. 1993. Immunity to intracellular bacteria. *Annu. Rev. Immunol.* 11:129.
5 Seki, E., Tsutsui, H., Tsuji, N. M. *et al.* 2002. Critical roles of myeloid differentiation factor 88-dependent proinflammatory cytokine release in early phase clearance of *Listeria monocytogenes* in mice. *J. Immunol.* 169:3863.
6 Takeda, K., Kaisho, T. and Akira, S. 2003. Toll-like receptors. *Annu. Rev. Immunol.* 21:335.
7 Akira, S., Uematsu, S. and Takeuchi, O. 2006. Pathogen recognition and innate immunity. *Cell* 124:783.
8 Okamura, H., Tsutsui, H., Komatsu, T. *et al.* 1995. Cloning of a new cytokine that induces IFN-γ production by T cells. *Nature* 378:88.
9 Nakanishi, K., Yoshimoto, T., Tsutsui, H. and Okamura, H. 2001. Interleukin-18 regulates both Th1 and Th2 responses. *Annu. Rev. Immunol.* 19:423.
10 Tsutsui, H., Yoshimoto, T., Hayashi, N., Mizutani, H. and Nakanishi, K. 2004. Induction of allergic inflammation by interleukin-18 in experimental animal models. *Immunol. Rev.* 202:115.
11 Adachi, O., Kawai, T., Takeda, K. *et al.* 1998. Targeted disruption of the MyD88 gene results in loss of IL-1- and IL- 18-mediated function. *Immunity* 9:143.
12 Kawai, T., Adachi, O., Ogawa, T., Takeda, K. and Akira, S. 1999. Unresponsiveness of MyD88-deficient mice to endotoxin. *Immunity* 11:115.
13 Wang, W., Tanaka, T., Okamura, H. *et al.* 2001. Interleukin-18 enhances the production of interleukin-8 by eosinophils. *Eur. J. Immunol.* 31:1010.
14 Leung, B. P., Culshaw, S., Gracie, J. A. *et al.* 2001. A role for IL-18 in neutrophil activation. *J. Immunol.* 167:2879.
15 Rossi, D. and Zlotnik, A. 2000. The biology of chemokines and their receptors. *Annu. Rev. Immunol.* 18:212.
16 Takeuchi, O., Hoshino, K., Kawai, T. *et al.* 1999. Differential roles of TLR2 and TLR4 in recognition of gram-negative and gram-positive bacterial cell wall components. *Immunity* 11:443.
17 Hemmi, H., Kaisho, T., Takeuchi, O. *et al.* 2002. Small antiviral compounds activate immune cells via TLR7 MyD88-dependent signalling pathway. *Nat. Immunol.* 3:196.
18 Heil, F., Ahmad-Nejad, P., Hemmi, H. *et al.* 2003. The toll-like receptor 7 (TLR7)-specific stimulus loxoribine uncovers a strong relationship within the TLR7, 8 and 9 subfamily. *Eur. J. Immunol.* 33:2987.
19 Tsutsui, H., Matsui, K., Kawada, N. *et al.* 1997. IL-18 accounts for both TNF-α- and Fas ligand-mediated hepatotoxic pathways in endotoxin-induced liver injury in mice. *J. Immunol.* 159:3961.
20 Nakagawa, R., Naka, T., Tsutsui, H. *et al.* 2002. SOCS-1 participates in negative regulation of LPS response. *Immunity* 17:677.
21 Kaisho, T., Tsutsui, H., Tanaka, T. *et al.* 1999. Impairment of natural killer cytotoxic activity and interferon gamma production in CCAAT/enhancer binding protein gamma-deficient mice. *J. Exp. Med.* 190:1573.
22 Shimoda, K., Tsutsui, H., Aoki, K. *et al.* 2002. Partial impairment of interleukin-12 (IL-12) and IL-18 signaling in Tyk2-deficient mice. *Blood* 99:2094.
23 Tsutsui, H., Kayagaki, N., Kuida, K. *et al.* 1999. Caspase-1-independent, Fas/Fas ligand-mediated IL-18 secretion from macrophages causes acute liver injury in mice. *Immunity* 11:359.
24 Hyodo, Y., Matsui, K., Hayashi, N. *et al.* 1999. IL-18 up-regulates perforin-mediated NK activity without increasing perforin messenger RNA expression by binding to constitutively expressed IL-18 receptor. *J. Immunol.* 162:1662.
25 Seki, E., Tsutsui, H., Iimuro, Y. *et al.* 2005. Contribution of toll-like receptor/myeloid differentiation factor 88 signaling to murine liver regeneration. *Hepatology* 41:443.
26 Nagai, Y., Akashi, S., Nagafuku, M. *et al.* 2002. Essential role of MD-2 in LPS responsiveness and TLR4 distribution. *Nat. Immunol.* 3:667.
27 Jiang, Z., Georgel, P., Du, X. *et al.* 2005. CD14 is required for MyD88-independent LPS signaling. *Nat. Immunol.* 6:565.
28 Takeda, K., Tsutsui, H., Yoshimoto, T. *et al.* 1998. Defective NK cell activity and Th1 response in IL-18-deficient mice. *Immunity* 8:383.
29 Shimoda, K., Kato, K., Aoki, K. *et al.* 2000. Tyk2 plays a restricted role in IFN-α signaling, although it is required for IL-12-mediated T cell function. *Immunity* 13:561.
30 Nakahira, M., Ahn, H.-J., Park, W.-R. *et al.* 2002. Synergy of IL-12 and IL-18 for IFN-γ gene expression: IL-12-induced STAT4 contributes to IFN-γ promoter activation by up-regulating the binding activity of IL-18-induced activator protein 1. *J. Immunol.* 168:1146.
31 Yang, J., Zhu, H., Murphy, T. L., Ouyang, W. and Murphy, K. M. 2001. IL-18-stimulated GADD45β required in cytokine-induced, but not TCR-induced, IFN-γ production. *Nat. Immunol.* 2:157.
32 Salazar-Mather, T. P., Hamilton, T. A. and Biron, C. A. 2000. A chemokine-to-cytokin-to-chemokine cascade critical in antiviral defense. *J. Clin. Invest.* 105:985.

33 Dorner, B. G., Scheffold, A., Rolph, M. S. *et al.* 2002. MIP-1α, MIP-1β, RANTES, and ATAC/lymphotactin function together with IFN-γ as type 1 cytokines. *Proc. Natl Acad. Sci. USA* 99:6181.
34 Dorner, B. G., Smith, H. R.C., French, A. R. *et al.* 2004. Coordinate expression of cytokines and chemokines by NK cells during murine cytomegalovirus infection. *J. Immunol.* 172:3119.
35 Salazar-Mather, T. P., Orange, J. S. and Biron, C. A. 1998. Early murine cytomegalovirus (MCMV) infection induces liver natural killer (NK) cell inflammation and protection through macrophage inflammatory protein 1α (MIP-1α)-dependent pathway. *J. Exp. Med.* 187:1.
36 Mack, M., Cihak, J., Simonis, C. *et al.* 2001. Expression and characterization of the chemokine receptors CCR2 and CCR5 in mice. *J. Immunol.* 166:4697.
37 Tyner, J. W., Uchida, O., Kajiwara, N. *et al.* 2005. CCL5-CCR5 interaction provides antiapoptotic signals for macrophage survival during viral infection. *Nat. Med.* 11:1180.
38 Ank, N., Petersen, K., Malmgaard, L., Mogensen, S. C. and Paludan, S. R. 2005. Age-dependent role for CCR5 in antiviral host defense against herpes simplex virus type 2. *J. Virol.* 79:9831.
39 Ortaldo, J. R., Bere, E. W., Hodge, D. and Young, H. A. 2001. Activating Ly-49 NK receptors: Central role in cytokine and chemokine production. *J. Immunol.* 166:4994.
40 Salazar-Mather, T., Lewis, C. A. and Biron, C. A. 2002. Type I interferons regulate inflammatory cell trafficking and macrophage inflammatory protein 1α delivery to the liver. *J. Clin. Invest.* 110:321.
41 Nakahira, M., Tomura, M., Iwasaki, M. *et al.* 2001. An absolute requirement for STAT4 and a role for IFN-γ as an amplifying factor in IL-12 induction for the functional IL-18 receptor complex. *J. Immunol.* 167:1306.
42 Tsutsui, H., Nakanishi, K., Matsui, K. *et al.* 1996. Interferon-gamma-inducing factor up-regulates Fas ligand-mediated cytotoxic activity of murine natural killer cell clones. *J. Immunol.* 157:3967.
43 Hornung, V., Rothenfusser, S., Britsch, S. *et al.* 2002. Quantitative expression of toll-like receptor 1-10 mRNA in cellular subsets of human peripheral blood mononuclear cells and sensitivity to CpG oligodeoxynucleotides. *J. Immunol.* 168:4531.
44 Chalifour, A., Jeannin, P., Gauchat, J.-F., Blaecke, A., Malissard, M. and N'Guyen, T. 2004. Direct bacterial protein PAMP recognition by human NK cells involves TLRs and triggers α-defensin production. *Blood* 104:1778.
45 Sivori, S., Falco, M., Della Chiesa, M., Citale, M., Moretta, L. and Moretta, A. 2004. CpG and double-stranded RNA trigger human NK cells by toll-like receptors: Induction of cytokine release and cytotoxicity against tumors and dendritic cells. *Proc. Natl Acad. Sci. USA* 101:10116.
46 Schmidt, K. N., Leung, B., Kwong, M. *et al.* 2004. APC-independent activation of NK cells by the toll-like receptor 3 agonist double-stranded RNA. *J. Immunol.* 172:138.

T helper 1 cells stimulated with ovalbumin and IL-18 induce airway hyperresponsiveness and lung fibrosis by IFN-γ and IL-13 production

Nobuki Hayashi*†, Tomohiro Yoshimoto*†, Kenji Izuhara‡, Kiyoshi Matsui§, Toshio Tanaka¶, and Kenji Nakanishi*†‖

*Departments of Immunology and Medical Zoology and §Internal Medicine, Hyogo College of Medicine, Nishinomiya, Hyogo 663-8501, Japan; ‡Division of Medical Biochemistry, Department of Biomedical Science, Saga Medical School, Saga 849-8501, Japan; ¶Department of Molecular Medicine, Osaka University Graduate School of Medicine, Suita, Osaka 565-0871, Japan; and †Collaborative Development of Innovation Seeds, Japan Science and Technology Corporation, Tokyo 102-8666, Japan

Communicated by Mark M. Davis, Stanford University School of Medicine, Stanford, CA, July 27, 2007 (received for review October 6, 2006)

We previously reported that ovalbumin (OVA) and IL-18 nasally administered act on memory type T helper (Th)1 cells to induce airway hyperresponsiveness (AHR) and inflammation, which is characterized by peribronchial infiltration with neutrophils and eosinophils. Here, we report this administration also induces lung fibrosis in an IL-13-dependent manner. Th1 cells secrete several cytokines, including IFN-γ and bronchogenic cytokine IL-13, when stimulated with antigen (Ag) and IL-18. However, IL-13 blockade failed to attenuate AHR, although this treatment inhibited eosinophilic infiltration. To understand the mechanism by which Th1 cells induce AHR after Ag plus IL-18 challenge, we established "passive" and "active" Th1 mice by transferring OVA-specific Th1 cells into naïve BALB/c mice or by immunizing naïve BALB/c mice with OVA/complete Freund's adjuvant, respectively. Administration of Ag and IL-18 induced both types of Th1 mice to develop AHR, airway inflammation, and lung fibrosis. Furthermore, this treatment induced deposition of periostin, a novel component of lung fibrosis. Neutralization of IL-13 or IFN-γ during Ag plus IL-18 challenges inhibited the combination of eosinophilic infiltration, lung fibrosis, and periostin deposition or the combination of neutrophilic infiltration and AHR, respectively. We also found that coadministration of OVA and LPS into Th1 mice induced AHR and airway inflammation via endogenous IL-18. Thus, IL-18 becomes a key target molecule for the development of a therapeutic regimen for the treatment of Th1-cell-induced bronchial asthma.

bronchial asthma | LPS | periostin | hydroxy proline | airway inflammation

Bronchial asthma is a complex syndrome characterized by airway hyperresponsiveness (AHR) and reversible airflow obstruction associated with airway inflammation and remodeling and occasional high serum level of IgE (1–7). Histologically, there are infiltrates of eosinophils, degranulated mast cells, subbasement membrane thickening, hyperplasia and hypertrophy of bronchial smooth muscle, and hyperplasia of airway goblet cells (1, 2). Th2 cells have been recognized as inducing bronchial asthma by production of Th2 cytokines (1–12). Particularly, IL-13 is suggested to play a critical role in induction of AHR, eosinophilic infiltration, goblet cell metaplasia, and lung fibrosis (9–13). In contrast, Th1 cells previously had been regarded to inhibit bronchial asthma by virtue of IFN-γ (14–16). However, several studies have disclosed the disability of Th1 cell to suppress Th2 cell-induced AHR (17–21). Moreover, a combination of Th1 and Th2 cells or their products augment each activity to induce airway inflammation and AHR (17, 18, 21). Thus, bronchial asthma is a complicated disease induced by the functions of Th1 and Th2 cells.

Recently, we have demonstrated that antigen (Ag) plus IL-18 acts on adoptively transferred memory type Th1 cells to induce airway inflammation and AHR in a naïve host mouse (22). These Th1 cells express ovalbumin (OVA)-specific T cell antigen receptor and IL-18 receptor (22, 23). They produce IFN-γ in response to OVA and increase further IFN-γ production in response to additional IL-18 stimulation (22, 23). Most surprisingly, they simultaneously produce Th2 cytokines (e.g., IL-9 and IL-13), granulocyte–macrophage colony-stimulating factor and chemokines (e.g., RANTES and macrophage inflammatory protein 1α) when stimulated with OVA and IL-18 (22). Human Th1 cells also produce Th1 and Th2 cytokines and IL-8 in response to anti-CD3 plus IL-18 (24). Recently, we demonstrated Th1 cells induce intrinsic atopic dermatitis by production of Th1 and Th2 cytokines and chemokines (25). Thus, IL-18 has added its new function to its growing functional list (26–29). Based on this unique function of Ag- plus IL-18-stimulated Th1 cells, we proposed to designate them as "super Th1 cells" (25). It is important to determine the mechanism by which super Th1 cells induce bronchial asthma by production of both Th1 and Th2 cytokines. However, as we reported previously (22), IL-13 blockade fails to attenuate Ag- plus IL-18-induced AHR, although this treatment markedly diminishes eosinophilic infiltration. These results prompted us to examine the role of Th1 cytokine in induction of AHR and airway inflammation.

In our previous report, we established "passive Th1 mice" by transferring OVA-specific memory Th1 cells (1×10^7 cells per mouse) into naïve BALB/c mice (22). Here, we prepared "active Th1 mice" by immunizing BALB/c mice with OVA in complete Freund's adjuvant (CFA) 2 weeks before experimentation. Both types of Th1 mice develop AHR, airway inflammation, and lung fibrosis after challenge with OVA and IL-18. Furthermore, they express periostin, a novel component of lung fibrosis under the control of IL-4 and IL-13 signals (30). Administration of anti-IFN-γ Ab almost completely inhibited AHR and neutrophilic infiltration, whereas IL-13 neutralization inhibited lung fibrosis and eosinophilic infiltration without affecting AHR. Thus, Th1 cells become very harmful super Th1 cells when stimulated with OVA and IL-18 by production of IFN-γ and IL-13 in the lungs. Of interest, OVA/CFA-immunized mice develop AHR and airway inflammation upon challenge with OVA and LPS via endogenous IL-18. Importantly, administration of anti-IL-18 almost completely inhibited this OVA/LPS-induced AHR, thereby rationalizing the development of reagents that down-regulate IL-18 for the treatment of Th1-cell-induced bronchial asthma.

Author contributions: N.H. and K.N. designed research; N.H. and T.Y. performed research; K.I. contributed new reagents/analytic tools; T.Y., K.I., K.M., and T.T. analyzed data; and K.N. wrote the paper.

The authors declare no conflict of interest.

Abbreviations: Ag, antigen; AHR, airway hyperresponsiveness; BALF, bronchoalveolar lavage fluid; Cdyn, dynamic compliance; CFA, complete Freund's adjuvant; OVA, ovalbumin; Th, T helper.

‖To whom correspondence should be addressed at: Department of Immunology and Medical Zoology, Hyogo College of Medicine, 1-1 Mukogawa-cho, Nishinomiya, Hyogo 663-8501, Japan. E-mail: nakaken@hyo-med.ac.jp.

This article contains supporting information online at www.pnas.org/cgi/content/full/0706378104/DC1.

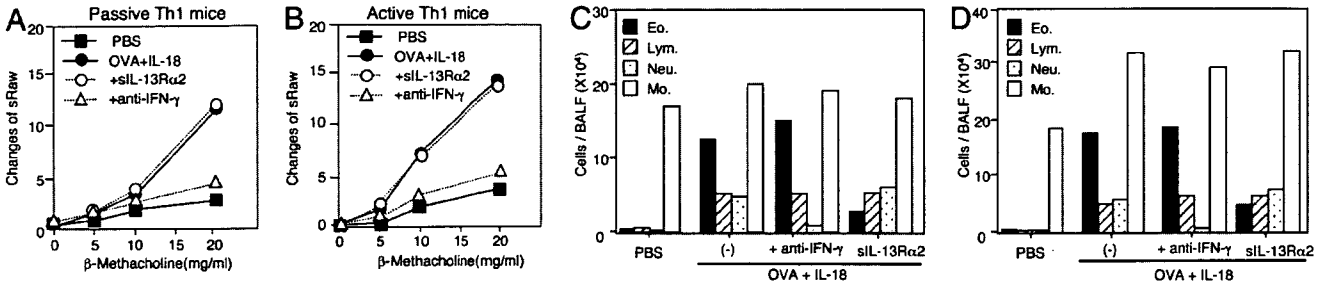

Fig. 1. Anti-IFN-γ Ab treatment protected against Ag- plus IL-18-induced AHR and accumulation of neutrophils in Th1 mice. Passive (*A* and *C*) and active (*B* and *D*) Th1 mice were exposed to daily intranasally administered PBS (50 μl) or OVA (100 μg per 50 μl of PBS) plus IL-18 (0.5 μg per 50 μl of PBS) for 3 days. A total of 20 μg of sIL-13Rα$_2$-Fc chimera (sIL13Rα2) was used for IL-13 blockade *in vivo*. For the blockade of IFN-γ *in vivo*, 50 μg of anti-IFN-γ Ab was intranasally coadministered with OVA and IL-18 for 3 days. (*A* and *B*) At 24 h after the final exposure to OVA plus IL-18, AHR in response to increased concentrations of inhaled β-methacholine and inflammatory cell composition of BALF was examined. (*C* and *D*) Cell differential percentages were determined by light microscopic evaluation of cytospin preparation. Representative results of five to seven animals per group are shown.

Results

OVA and IL-18 Induce AHR in Th1 Cell-Bearing Mice in an IFN-γ-Dependent Manner. We previously reported that mice receiving memory Th1 cells develop AHR and airway inflammation after intranasal administration of OVA and IL-18 (22). Th1 cells produce IFN-γ, IL-9, IL-13, granulocyte–macrophage colony-stimulating factor, and chemokines in response to Ag, IL-2, and IL-18 *in vitro* (22, 25). Among the cytokines produced, IL-13 is most bronchogenic and participates in AHR (7–13). However, neutralization of IL-13 in the lungs fails to inhibit Th1-cell-induced AHR (22). Thus, we sought to determine the causative factor critically involved in this Th1-cell-induced AHR.

We first examined the relevant role of IFN-γ in induction of bronchial asthma. For this purpose, we constructed a convenient Th1-cell-induced bronchial asthma model. We immunized BALB/c mice with OVA in CFA (OVA/CFA) to actively induce OVA-specific Th1 cells *in vivo*. Indeed, this treatment strongly induced OVA-specific Th1 cells *in vivo* [supporting information (SI) Fig. 8*A*]. We designated these OVA/CFA-primed mice as active Th1 mice and tested their development of bronchial asthma after their nasal exposure to OVA and IL-18. We compared their responses to those of naïve mice receiving adoptively transferred OVA-specific Th1 cells (passive Th1 mice). As shown in Fig. 1*A* and *B*, both types of Th1 mice developed AHR. Consistent with our previous report (22), each stimulus alone did not induce AHR (SI Fig. 8*B*). Furthermore, both noninvasive and invasive measurements of AHR provided basically identical results, excluding a contribution from the upper airway component to the induction of AHR (Fig. 2). Invasive measurement also indicated that OVA- plus IL-18-challenged Th1 mice reduced lung compliance. Bronchoalveolar lavage fluid (BALF) examination revealed that administration of OVA and IL-18 induced increases in the numbers of eosinophils, lymphocytes, and neutrophils in Th1-cell-bearing mice (Fig. 1 *C* and *D*) but not in normal control mice (SI Fig. 8*C*) (22). Therefore, both active and passive Th1 mice showed similar responses to OVA plus IL-18 in terms of AHR and airway inflammation.

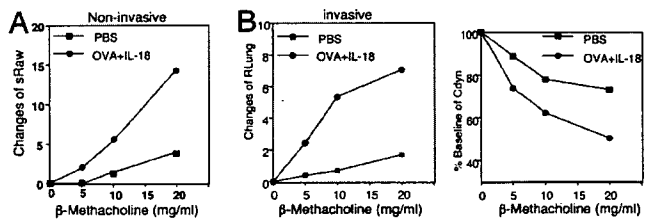

Fig. 2. Noninvasive or invasive measurement of Ag- plus IL-18-induced AHR. Active Th1 mice were exposed daily to intranasal administration of PBS (50 μl) or OVA (100 μg per 50 μl of PBS) plus IL-18 (0.5 μg per 50 μl of PBS) for 3 days. At 24 h after the final exposure to OVA plus IL-18, AHR in response to increased concentrations of inhaled β-methacholine was determined by noninvasive [specific airway resistance (sRaw)] (*A*) and invasive [pulmonary resistance (RLung) and Cdyn] (*B*) measurement. Baseline values for pulmonary resistance ($cmH_2O/ml \cdot sec^{-1}$) and Cdyn (ml/cmH_2O) were 4.58 for PBS, 4.65 for OVA plus IL-18, 0.0119 for PBS, and 0.0133 for OVA plus IL-18. Representative results of five to seven animals per group are shown.

To evaluate the effects of IFN-γ and IL-13 on AHR and airway inflammation, we treated Th1 mice with an Ab against IFN-γ or sIL-13Rα$_2$-Fc chimera (sIL-13Rα2). As shown in Fig. 1 *A* and *B*, neutralization of IFN-γ almost completely inhibited Ag- plus IL-18-induced AHR, whereas neutralization of IL-13 failed to do so, suggesting a contribution from IFN-γ but not from IL-13 to the induction of AHR. Nevertheless, this IL-13 neutralization inhibited eosinophilic infiltration, excluding a contribution from eosinophilic infiltration to the induction of AHR in Th1-cell-induced bronchial asthma. To understand the mechanism whereby only IFN-γ neutralization inhibited AHR in both types of Th1 mice, we compared the cellular components in BALFs from Th1 mice either receiving these treatments or not. As shown in Fig. 1 *C* and *D*, neutralization of IFN-γ or IL-13 selectively diminished neutrophilic or eosinophilic infiltration, respectively, suggesting their differential regulation by IFN-γ and IL-13.

Histological analysis revealed that both types of Th1 mice expressed peribronchial and perivenular infiltrations composed mainly of eosinophils and neutrophils after OVA plus IL-18 treatment (Fig. 3). The degree of eosinophilic infiltrations in the lungs of the Th1-cell-bearing mice is comparable to that of Th2-cell-bearing mice after exposure to OVA (22). Consistent with the result of Fig. 1 *C* and *D*, neutralization of IFN-γ and IL-13 appeared to reduce more selectively neutrophilic and eosinophilic infiltrations in the lungs, respectively (Fig. 3). These results strongly indicated that Th1 cells induce AHR and eosinophilic infiltration in response to Ag and IL-18 by production of IFN-γ and IL-13, respectively.

IL-4Rα$^{-/-}$ Mice Normally Develop Bronchial Asthma After OVA Plus IL-18 Challenge. It is important to exclude entirely the contribution from IL-13 to AHR because residual IL-13 might collaborate with IFN-γ for the induction of AHR. For this purpose, we primed BALB/c background IL-4Rα$^{-/-}$ mice with OVA/CFA and subsequently challenged them with OVA and IL-18. As expected, IL-4Rα$^{-/-}$ mice normally developed AHR (Fig. 4*A*), which formally excluded a contribution from IL-13 to the induction of AHR in Th1-cell-bearing mice.

We simultaneously examined the cell components in the BALFs (Fig. 4*B*). We also performed histological evaluation of the lungs (Fig. 4*C*). As expected from the BALFs, results of sIL-13Rα2-treated mice (Fig. 1 *C* and *D*), OVA/CFA-primed, and OVA/IL-18-challenged IL-4Rα$^{-/-}$ mice markedly reduced the numbers of

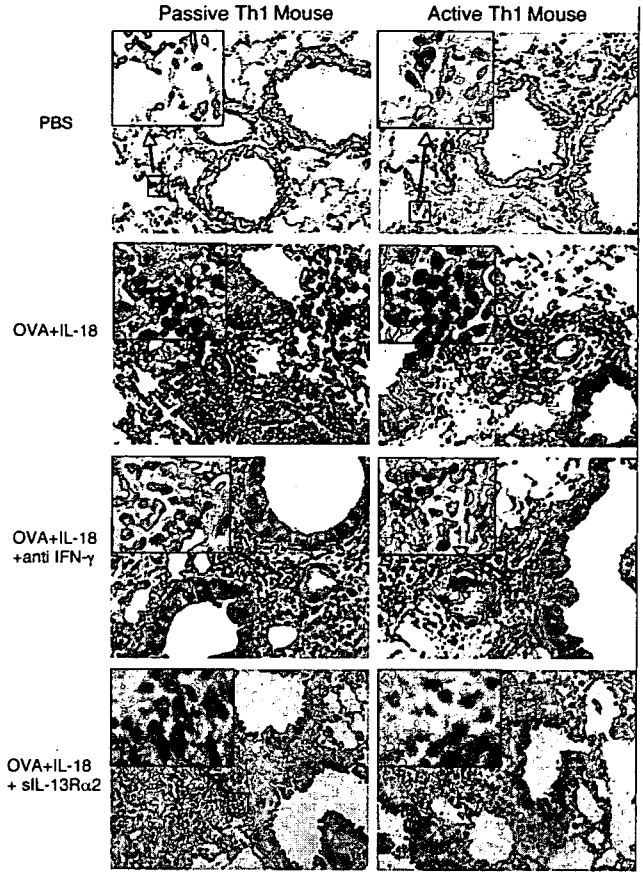

Fig. 3. Histological examination of the lung tissues from Th1 mice exposed to OVA and IL-18. Both passive and active Th1 mice were exposed daily to intranasally administered PBS or OVA plus IL-18 with anti-IFN-γ or sIL-13Rα2 as described in the legend of Fig. 1. At 24 h after final exposure, lungs from each group of mice were prepared for histological examination by perfusing the animal via the right ventricle with 10 ml of PBS; the lungs were then fixed in formalin, cut into 3-μm sections, and stained with H&E as described in *Material and Methods*. [Original magnification, ×40 (*Insets*, ×200).]

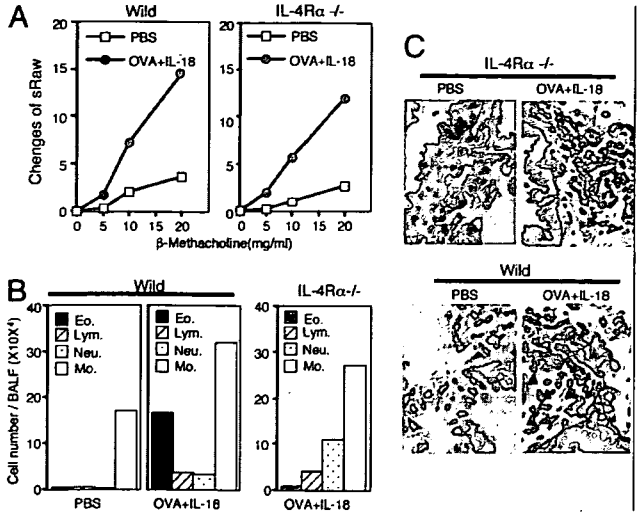

Fig. 4. IL-4Rα$^{-/-}$ mice often developed Th1-cell-induced AHR. BALB/c WT or BALB/c background IL-4Rα$^{-/-}$ mice, which were immunized with OVA in CFA 2 weeks previously, were exposed to daily intranasal administration of PBS or OVA plus IL-18 for 3 days. At 24 h after final exposure, the mice were analyzed for β-methacholine-induced AHR (*A*) and BALF (*B*) and their histological changes (*C*), as described for in the legends of Figs. 1 and 2. White arrowhead, neutrophil; black arrowhead, eosinophil. Representative results obtained from five to seven animals per group are shown. (Magnification, ×200.)

eosinophils and, conversely, increased the number of neutrophils in their BALFs (Fig. 4*B*). Histological examination revealed that OVA and IL-18 induced peribronchial infiltration in all cases of WT mice, as well as IL-4Rα$^{-/-}$ mice (Fig. 4*C*). However, compared with WT mice, IL-4Rα$^{-/-}$ mice markedly increased the cell infiltrates composed mainly of neutrophils (Fig. 4*C*), substantiating further the differential induction of neutrophils and eosinophil by IFN-γ and IL-13, respectively. Thus, IL-13 is not required for the induction of AHR in OVA- plus IL-18-administered Th1 mice.

Coadministration of Ag and LPS Induces AHR in Th1-Immunized Mice. Patients with bronchial asthma often develop AHR and airway inflammation after viral or bacterial infection (2, 31–33). It has been reported that infected animals often display an increase in serum levels of IL-18 after viral or bacterial infection (27). Thus, we assumed that pathogen or pathogen-associated molecular pattern might induce AHR by the induction of IL-18. To examine this possibility, we treated Th1 mice with intranasal administration of OVA and LPS instead of OVA and IL-18. We found that mice receiving such treatment developed AHR and severe airway inflammation (Fig. 5 *A* and *B*).

We next tried to determine whether OVA and LPS induced AHR by the action of endogenous IL-18 that, in turn, induces IFN-γ production from Th1 cells. Thus, we examined the capacity of anti-IL-18 or anti-IFN-γ Ab treatment to inhibit this OVA plus LPS-induced AHR (Fig. 5). Each Ab treatment markedly diminished AHR (Fig. 5*A*). Furthermore, IFN-γ$^{-/-}$ or IL-18$^{-/-}$ mice were resistant to the sequential treatment with OVA/CFA priming and OVA/LPS challenge (Fig. 5*C*), substantiating further the importance of IL-18-dependent IFN-γ production for AHR. However, this OVA plus LPS challenge only increased the number of neutrophils in BALFs (Fig. 5*B*). Thus, OVA plus LPS partially replaced the action of OVA and IL-18. However, anti-IFN-γ Ab treatment modestly increased the number of eosinophils and lymphocytes but markedly reduced the number of neutrophils (Fig. 5*B*). These results strongly indicated that OVA plus LPS induced Th1 cells to produce IFN-γ via endogenous IL-18, resulting in induction of neutrophilic infiltration and inhibition of eosinophilic infiltration.

Ag- and IL-18-Induced Lung Fibrosis Depends on Endogenous IL-13. IL-13 is indispensable for eosinophilic inflammation (7, 9–13, 34). Furthermore, IL-13 has the potential to induce lung fibrosis by activating macrophages, bronchoepithelial cells, and eosinophils to produce fibrogenic cytokine TGF-β (35, 36). Therefore, we tested the pathological effect of IL-13 derived from Ag- plus IL-18-stimulated Th1 cells on lung fibrosis. We compared the degree of lung fibrosis in the lungs of Th1 and Th2 mice after challenge with OVA plus IL-18 or OVA alone, respectively. Both Th1 and Th2 mice similarly developed lung fibrosis (Fig. 6). Development of fibrosis was proven to depend on the function of endogenous IL-13 because blockade of endogenous IL-13 inhibited lung fibrosis (Fig. 6 *Ad* and *Bh*). Thus, OVA- plus IL-18-stimulated Th1 cells or OVA-stimulated Th2 cells induced lung fibrosis by production of IL-13.

To examine further the extent of fibrosis, we measured the lung hydroxyproline content (Table 1). Th1 mice challenged with OVA plus IL-18 significantly increased hydroxyproline content in their lungs, whereas Th1 mice challenged identically but under IL-13 neutralization conditions did not, indicating that IL-18 induces lung fibrosis by acting on Th1 cells to produce IL-13. Furthermore, anti-IFN-γ Ab treatment did not affect lung hydroxyproline content

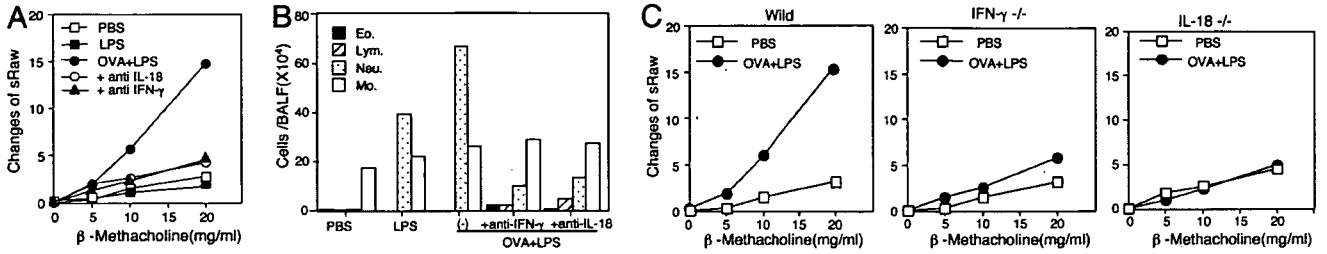

Fig. 5. Neutralization of IFN-γ or IL-18 abolished OVA plus LPS-induced AHR and neutrophilic infiltration in active Th1 mice. BALB/c WT mice or BALB/c background IFN-$\gamma^{-/-}$ or IL-$18^{-/-}$ mice immunized with OVA/CFA 2 weeks previously were challenged intranasally with 5 μg of LPS and 100 μg of OVA. To block endogenous IL-18 or IFN-γ, Ab against IL-18 or IFN-γ mixed with OVA and LPS was coadministered daily. At 24 h after final administration, β-methacholine-induced AHR (*A* and *C*) and cell population in BALF (*B*) were analyzed as described in the legend of Fig. 1. Representative results of five to seven animals per group are shown. The results shown in *A Left* and *C Left* were obtained from the same experiment.

in OVA- plus IL-18-challenged Th1 mice. These results allowed us to conclude that IL-18 induces lung fibrosis by the induction of endogenous IL-13.

We finally examined the expression of periostin, a novel component of lung fibrosis developing at the early stage of bronchial asthma and colocalizing with the extracellular matrix protein involved in lung fibrosis (30). Induction of periostin is shown to depend on IL-4 and IL-13 but not TGF-β signaling (30). OVA/CFA-primed mice expressed this molecule in response to OVA plus IL-18 challenge (Fig. 7). IL-13 blockade inhibited this expression, suggesting that Th1 cells induce lung fibrosis and periostin deposition by production of IL-13 (Fig. 7). In conclusion, after being stimulated with Ag and IL-18, Th1 cells became very pathological super Th1 cells, which induce AHR and lung fibrosis by production of IFN-γ and IL-13, respectively, in this mouse model of bronchial asthma.

Discussion

We have established passive and active Th1 mice by transferring OVA-specific Th1 cells into or OVA/CFA immunization of naïve BALB/c mice, respectively. Both types of Th1 mice developed AHR and airway inflammation associated with lung fibrosis after intranasal challenge with OVA and IL-18. BALF analysis and histological evaluation revealed that they increased the number of eosinophils, neutrophils, and lymphocytes in their lungs (Figs. 1 and 3). Infiltrations of eosinophils and neutrophils in the lungs are regulated differentially by IL-13 and IFN-γ (Figs. 1 and 3). Results from IL-4Rα$^{-/-}$ mice excluded the potential contribution from IL-13 to Th1-cell-induced AHR (Fig. 4). Results from anti-IFN-γ-treated mice revealed that IFN-γ is a true causative factor responsible for inducing AHR (Fig. 1). OVA plus LPS replaced partly the effect of OVA and IL-18 by the induction of endogenous IL-18 (Fig. 5). We also showed that, like Th2 mice challenged with OVA, Ag- plus IL-18-challenged Th1 mice develop lung fibrosis associated with periostin deposition and increased lung hydroxyproline content, which are induced by the action IL-13 (Table 1 and Figs. 6 and 7). Thus, Th1 cells become very pathological super Th1 cells when stimulated with Ag and IL-18 by the production of IFN-γ and IL-13, which in combination induce AHR, peribronchial inflammation, and lung fibrosis in this mouse model of bronchial asthma.

It is well defined that the immunological situation toward Th1 cell development protects Th2 cell development and vice versa (14–16). Thus, the concept of Th1/Th2 development has been believed to be a dichotomy. However, our previous studies have clearly demonstrated that IL-18 disrupts the biologically reciprocal actions of Th1 and Th2 cells in mice (22, 24, 25). We showed that OVA-specific monoclonal Th1 cells, which we developed *in vitro*, have the potential to produce Th1 cytokine (IFN-γ) and Th2 cytokine (IL-9, IL-13) as well as chemokines (e.g., RANTES and macrophage inflammatory protein 1α) in response to Ag, IL-2, and IL-18 *in vitro* (22, 25). Thus, Ag- and IL-18-stimulated Th1 cells produce a similar spectrum of cytokines and chemokines that are produced by activated mast cells. In this study, we first examined whether OVA-specific Th1 cells, which we newly developed *in vivo* by immunization of mice with OVA/CFA, can produce IFN-γ, IL-9, IL-13, granulocyte–macrophage colony-stimulating factor, and chemokines in response to Ag, IL-2 and IL-18 *in vitro*. Furthermore, we confirmed that they had such potential. Next, we examined whether OVA/CFA-immunized active Th1 mice developed AHR and airway inflammation after administration of OVA and IL-18. Consistent with our previous report obtained from passive Th1 mice (22), active Th1 mice exposed to OVA alone did not develop AHR (SI Fig. 8*B*). However, when nasally exposed to OVA and

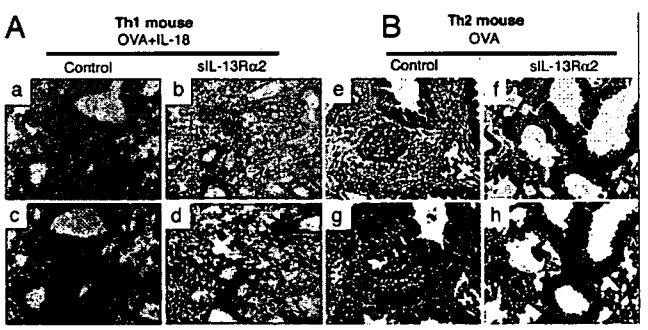

Fig. 6. IL-13-dependent lung fibrosis in Ag- plus IL-18-administered Th1 mice or Ag-administered Th2 mice. Active Th1 mice or Th2 were induced by immunization with OVA/CFA (*A*) or OVA/alum (*B*), respectively. Immunized mice were exposed daily to intranasally administered OVA or OVA plus IL-18 with or without sIL-13Rα2 as described in the legend of Fig. 1. At 24 h after final exposure, lungs from each group of mice were prepared, stained with H&E (*a*, *b*, *e*, and *f*) or Azan–Mallory (*c*, *d*, *g*, and *h*), and used for histological examination. (Original magnification, ×40.)

Table 1. Lung hydroxyproline level in active Th1 mice challenged with OVA plus IL-18

Active Th1 mouse	*n*	Hydroxyproline, μg per lung
PBS	4	110.17 ± 6.4
OVA + IL-18	4	149.9 ± 12.3*
OVA + IL-18 + sIL-13Rα2	4	118.48 ± 3.5
OVA + IL-18 + anti-IFNγ	4	158.83 ± 8.3†

Active Th1 mice were exposed daily to intranasal administration of PBS (50 μl), OVA (100 μg per 50 μl of PBS), or OVA (100 μg per 50 μl of PBS) plus IL-18 (0.5 μg per 50 μl of PBS) for 3 days. sIL-13Rα2 or anti-IFN-γ antibody was used for IL-13 or IFN-γ blocking, respectively, *in vivo*. At 24 h after the final exposure, lung total hydroxyproline levels were measured. *, $P < 0.01$ (vs. PBS treatment or OVA + IL-18 + sIL-13Rα2 treatment).
†Not significant (vs. OVA + IL-18 treatment).